The Chinese Silver Standard: Parity, Predictability, and (In)Stability, 1912–1934

Huachen Li[†] AND **James M. Nason**[‡]

January 31, 2024

Abstract

This paper assesses the debate about the demise of the Chinese silver standard in the mid 1930s. One side argues the U.S. Silver Purchase Act of June 1934 drained China of silver, which caused deflation and economic crises. A related claim is the Chinese silver standard was intrinsically unstable. These hypotheses are evaluated by estimating Bayesian structural VARs with drifting parameters on China-U.K. and China-U.S. samples from April 1912 to September 1934. We find instability in the Chinese silver standard peaked during the NBER recession of January 1920–July 1921 and the Great Depression (August 1929–March 1933). Hence, neither the U.S. Silver Purchase Act of June 1934 nor a design flaw lead to the end of the Chinese silver standard.

JEL Classification Number: $E42$, $F31$, $F33$, and $N25$.

Keywords: China; silver standard; exchange rate; parity deviation; Bayesian structural VAR.

[†] *e-mail*: li8@kenyon.edu, *website*: `https://sites.google.com/view/huachenli`, *affiliation*: Department of Economics, Ascension Hall, Kenyon College, Gambier, Ohio 43022.

[‡] *e-mail*: jmnason87@gmail.com, *website*: `https://www.jamesmnason.net`, *affiliations*: Centre for Applied Macroeconomic Analysis, Australian National University and Virginia Center for Economic Policy, University of Virginia.

Acknowledgments: We thank Gregor Smith for a useful conversation and participants in a session of the Midwest Macro Group meetings at Texas Tech University in November 2023. The online appendix for the paper is available at `https://www.jamesmnason.net/research`. All errors are our own.

1. INTRODUCTION

The Chinese economy ran on a commodity monetary standard linked to silver for hundreds of years before its end in the mid 1930s. By 1900, payments for regional trade within China were settled in local money markets each using its own unit of account denominated in *tael* (*liang* or Chinese ounce). Embedded in a local *tael* was a price for silver, but China took the world price of silver as given. As a result, it defined parity for the Chinese silver standard.

The Nanjing government replaced the Chinese silver standard with the *fabi* (fiat currency) in November 1935 (1935M11).[1] However, Leavens (1939, pp. 300–302) describes the Nanjing government as breaking the Chinese silver standard a year earlier. A customs duty on exports of silver was levied by the Nanjing government to reduce these flows in 1934M10. At the same time, it imposed an equalization charge (step-up duty) on silver exports and began a regime of managed exchange rates. The intent of the last two actions was to restore the Chinese silver standard to parity by moving the domestic price of silver closer to the world price. These policy tools were needed because beginning in 1934M10 the customs duty on exports of silver decoupled the Chinese silver standard from the world price of silver.

This paper studies two hypotheses that aim to explain the Nanjing government's motives for ending the Chinese silver standard. Friedman and Schwartz (1963), Chang (1988), Friedman (1992), Burdekin (2008), Silber (2019), and Dean (2020) claim the U.S. Silver Purchase Act passed by Congress in 1934M06 destabilized the Chinese silver standard. The Act instructed the U.S. Treasury to buy silver at greater than market prices. Hence, silver left China causing deflation, financial crises, and the policy responses of the Nanjing government starting in 1934M10.

[1]The Nanjing government substituted the *yuan* (Chinese silver dollar) for the *tael* in 1933M04. This was only a change in numeraire. Bratter (1933) notes that converting *yuan* into *tael* was at a known rate. Furthermore, banks continued to return silver for their notes and deposits on demand after 1933M04 until convertibility ceased when the *fabi* became legal tender in China.

Shiroyama (2008), Ho and Lai (2013), and Ho (2014) offer a related hypothesis that instability was built into the Chinese silver standard. They argue its fragility was accentuated by the U.S. Silver Purchase Act because parity for the Chinese silver standard was defined by the world price of silver. Hence, domestic fiscal and monetary policy could not smooth shocks that produced deviations from parity of the Chinese silver standard.

We evaluate the two hypotheses seeking to explain the demise of the Chinese silver standard by estimating structural VARs (SVARs) with time-varying parameters (TVPs) and stochastic volatility (SV) on China-U.K. and China-U.S. samples from 1912M04 to 1934M09. The estimates are engaged to construct tests of uncovered interest parity (UIP), the predictability and instability statistics of Cogley, Primiceri, and Sargent (2010) and Cogley and Sargent (2015), and impulse response functions (IRFs). This is the econometric evidence we use to judge whether the U.S. Silver Purchase Act or its inherent fragility lead the Chinese silver standard to fail.

The Chinese silver standard has been studied using econometric tools by Lai and Gau (2003), Burdekin (2008), Ho and Lai (2013, 2016), Ho, Lai, and Gau (2013), Ho (2014), Jacks, Yan, and Zhao (2017), Zhao and Zhao (2018), Ma and Zhao (2020), Palma and Zhao (2021), and Chen, Li, and Xie (2022). Our paper extends this literature in three ways. First, the Chinese silver standard is assessed on new China-U.K. and China-U.S. samples. Second, identification of the SVARs rests on the exchange rate-risk premium model of Engel (2016). Third, estimated TVP-SV-SVARs are used to construct monthly UIP tests, predictability and instability statistics, and IRFs that address the tumult China, the U.K., and U.S. experienced during the sample.

We compile samples in which China is the home country and the U.K. or U.S. is the foreign economy. The samples consist of the cross-country interest rate spread and inflation differential, i_t and π_t, deviation from parity of the Chinese silver standard, ρ_t, and currency return, Δe_t,

from 1912M04 to 1934M04. The measures of i_t and π_t have not been used before to study the Chinese silver standard to the best of our knowledge.[2] Market observers collected (the logs of) the world price of silver, SP_t, and exchange rate, e_t. Since SP_t and e_t were set in spot markets, e_t floated and $\rho_t = e_t - SP_t$ under the Chinese silver standard. We interpret this equation as an equilibrium relationship of the Chinese silver standard that equates its state to ρ_t. Viewing ρ_t this way likens the U.S. Silver Purchase Act of 1934M06 to a one-off risk premium shock that was internal to the China-U.S. sample, but was external to the China-U.K. sample.

Engel (2016) develops an exchange rate model in which a risk premium generates excess Δe_t. We use his model for two reasons. First, ρ_t corresponds to the risk premium. Second, solving Engel's model forward, appealing to the Beveridge and Nelson (1981) decomposition, applying a result in Nason and Rogers (2008), and assuming a reduced-form VAR generates i_t, π_t, ρ_t, and Δe_t yields a regression in which Δe_t responds to i_t, π_t, and ρ_t at impact. Our baseline SVAR rests on this regression and placing zeros on the nine off-diagonal impact coefficients in the i_t, π_t, and ρ_t regressions to identify globally international finance, cross-country nominal demand, risk premium, and trend exchange rate shocks. We also globally identify these shocks in 10 alternative SVARs that depart from the baseline by allowing different combinations of the off-diagonal impact coefficients in the π_t and ρ_t regressions to be free parameters.

The TVPs and SVs are included in the SVARs to handle the turmoil affecting China, the U.K., and U.S. from 1912 to 1935. China suffered political upheaval during these years. Important episodes were the Warlord Era, which began in 1916M06 and ended with the Northern Expedition of 1926M07–1928M12 that unified China under the Nanjing government, the Civil War starting in 1927M08, and the invasion of Manchuria by Japan in 1931M09. For the U.K. and

[2]Ho and Li (2014) use $i_{S,t}$ to study instability in the Shanghai government bond market of the 1920s and 1930s.

U.S, the First World War, its aftermath, and the Great Depression defined the era. These events drove changes in the underlying economic environment that are captured by TVPs and SV.

The two hypotheses studied by this paper are disputed by Brandt and Sargent (1989), Rawski (1993), Ho, Lai, and Gau (2013), and Chen, Li, and Xie (2022). Rawski shows China had inflation after passage of the Silver Purchase Act in 1934M06. Chen, Li, and Xie report estimates on pre-1935 data showing the lack of deflation stemmed from banks in China issuing notes backed by silver that replaced the missing commodity money. Ho, Lai, and Gau find e_t moved with SP_t on a pre-1934M10 sample. These papers indicate the Chinese silver standard was stable despite the turbulence it faced from the 1910s to the mid 1930s. Finally, Brandt and Sargent focus on two goals they argue animated the Nanjing government's actions from 1934M10 to introducing the *fabi* in 1935M11. The Nanjing government coveted the income generated in domestic and international money markets in China and sought to undo the constraints the Chinese silver standard imposed on domestic fiscal and monetary policy.

We draft the Metropolis in Gibbs Markov chain Monte Carlo (MCMC) sampler of Canova and Pérez Forero (2015) to estimate the TVP-SV-SVARs. Their MCMC sampler generate posterior distributions of a TVP-SV-SVAR identified on non-recursive restrictions, which describes several of our alternative identification schemes.

The estimated TVP-SV-SVARs yield little evidence the U.S. Silver Purchase Act of 1934M06 or intrinsic instability caused the Chinese silver standard to collapse. There are few rejections of UIP, SV and instability peak during the 1920M01–1921M07 recession and Great Depression, predictability starts to rise in the Great Depression if not earlier, and IRFs are nearly unchanged from 1934M01 to 1934M09. This leaves the actions the Nanjing government took beginning in 1934M10 as the remaining explanation for the demise of the Chinese silver standard.

The outline of the paper follows. Section 2 discusses the Chinese silver standard and data. The SVARs are constructed in section 3. Section 4 describes the TVP-SV-SVARs and Bayesian estimation methods. Results appear in sections 5 and 6. Section 7 concludes.

2. The Chinese Silver Standard and Its Data

This section reviews the Chinese silver standard and the China-U.K. and China-U.S. samples.

2.a. The Chinese silver standard

The only role a *tael* had in the Chinese silver standard was as a unit of account. Mediums of exchange in retail trade were copper, brass, and silver coins that had fractional claims on a *tael*; see Leavens (1939, pp. 87). Commercial and financial transactions were settled in local *tael* of which more than 170 existed by the early 1900s; see Dean (2020).

Of the unit of accounts that existed under the Chinese silver standard, Young (1931), Bratter (1933), Leavens (1939), Brandt, Ma, and Rawski (2014), Jacks, Yan, and Zhao (2017), and Ma (2019) contend the Shanghai *tael*, which dated to 1857, was preeminent by the 1910s. At the time the Republic of China was declared and Qing dynasty collapsed in early 1912, the bulk of China's international trade already flowed through the port of Shanghai. This helped Shanghai to become the hub of the most dynamic economy in China. As a result, the Shanghai *tael* came to dominate domestic and international economic and financial activity in China.

Domestic and international economic activity were supported by banks in Shanghai. They backed their notes and cleared domestic accounts with reserves held in silver ingots of about 50 Shanghai *taels* that were known as shoes of *sycee* (*i.e.*, fine silk); see Leavens (1939, p. 92).[3] Shanghai banks also exported shoes of *sycee* and imported silver denominated in Shanghai *tael*

[3]Converting a *tael* into a domestic price of silver was possible because, as Leavens (1939, pp. 91–95) discusses, weight and fineness (*i.e.*, grains of silver and fractional content of silver) defined a *tael*. In addition, Leavens notes the long time custom of the "Shanghai convention" converted the ideal *tael* into the Shanghai *tael*.

to settle international claims. Nevertheless, settling payments often prompted banks, given the state of their balance sheets, to trade reserves in an interbank market operated by the *Shanghai Qian Ye Gong Hui* (*i.e.*, Shanghai Banking Association).[4] Since the Shanghai interbank rate, $i_{S,t}$, cleared this market, it linked $i_{S,t}$ with foreign currency-Shanghai *tael* exchange rates, e_t.

The operating mechanism of the Chinese silver standard differed from the gold standard. A key reason was SP_t was set in a spot market in London or New York City (NYC).[5] Hence, SP_t defined parity for the Chinese silver standard and ρ_t was recovered by observing movements of e_t around SP_t. This mapped $\rho_t \gtreqless 0$ into overvaluation, parity, or undervaluation of the Shanghai *tael*. It is also useful to keep in mind that fluctuations in ρ_t reflected the equilibrium mechanism, $e_t - SP_t$, that restored the Chinese silver standard to parity.[6]

2.b. The China-U.K. and China-U.S. samples: 1912M04–1934M09

The founding of the Republic of China in 1912M01 and fall of the Qing dynasty the next month motivate us to begin the China-U.K. and China-U.S. samples in 1912M04. The samples end in 1934M09. The following month, the Nanjing government severed the link between e_t and SP_t; see Leavens (1939, pp. 300–302) and Ho, Lai, and Gau (2013).

Figure 1 plots the China-U.K. and China-U.S. samples, $y_t = [i_t \;\; \pi_t \;\; \rho_t \;\; \Delta e_t]'$, from 1912M04 to 1934M09, $T = 270$. From left to right and top to bottom, the panels contain plots of i_t, π_t, ρ_t, and Δe_t. China-U.K. variables are dot-dashed (red) lines, dotted (blue) lines are China-U.S. variables, and NBER recession dates are vertical gray bars. Appendix A1 reviews the methods used to compile the data shown in figure 1, but summaries of i_t, π_t, ρ_t, and Δe_t follow.

[4]When the Nanjing government nationalized the large Shanghai banks in 1935M04, their interbank market closed.
[5]The world silver market was in New York City from 1915M01 to 1934M08. London housed the world silver market from 1912M04 to 1914M12 and in 1934M09.
[6]This differs from the modern floating exchange rate regime in which the real exchange rate serves this purpose as, for example, in the vector error correction model estimated by Engel (2016).

INTEREST RATE SPREAD, i_t: Cross-country interest rate spreads are $i_t = i_{S,t} - i_{j,t}$, $j = UK, US$. *Zhongguo ren min yin hang Shanghai Shi fen hang* (1960) has monthly observations for the Shanghai interbank rate, $i_{S,t}$. Monthly money market rates for the U.K., $i_{UK,t}$, and U.S., $i_{US,t}$, are found in the NBER Macrohistory database.

INFLATION DIFFERENTIAL, π_t: Shanghai, U.K., and U.S. wholesale price indexes (WPIs) define inflation, $\pi_{m,t} = 100\left(p_{m,t} - p_{m,t-1}\right)$, where $p_{m,t} = \ln WPI_{m,t}$ and $m = S, UK, US$. The Shanghai Research Institute of Economics (1958) supplies monthly $WPI_{S,t}$ starting in 1922. Before 1922, Kong (1988) has an annual WPI for China. We compile a new $WPI_{S,t}$ from 1912M04 to 1934M09 by placing these WPIs on the same 1921 base year, interpolating the former into months, and splicing together these monthly WPIs at 1921M12–1922M01. The NBER Macrohistory database has monthly $WPI_{UK,t}$ and $WPI_{US,t}$. The WPIs yield $\pi_t = \pi_{S,t} - \pi_{j,t}$ for $j = UK, US$.

DEVIATIONS FROM PARITY, ρ_t: Observations on ρ_t from 1912M04 to 1933M12 are found in Wu (1935). We tap Ho and Lai (2016) for the last nine data points of the samples. Deviations from parity for the Chinese silver standard are $\rho_t = 100\left(e_{j/S,t} - SP_t\right)$, where $e_{j/S,t}$ is the log of the British pound (*GBP*)- or U.S. dollar (*USD*)-Shanghai *tael* exchange rate.

NOMINAL CURRENCY RETURNS, Δe_t: We obtain $e_{GBP/S,t}$ and $e_{USD/S,t}$ from Kong (1988). First differencing $e_{j/S,t}$ yields the currency return, $\Delta e_{j/S,t} = 100\left(e_{j/S,t} - e_{j/S,t-1}\right)$, $j = GBP, USD$.

3. AN EXCHANGE RATE-RISK PREMIUM SVAR

This section presents the exchange rate-risk premium model of Engel (2016), our baseline SVAR, and broadens it to 10 alternatives.

3.a. An exchange rate model with deviations from Chinese silver standard parity

The exchange rate-risk premium model of Engel (2016) is grounded in a concept of excess

currency returns linking deviations from parity for the Chinese silver standard, ρ_t, to a risk premium denominated in *tael* earned for holding deposits in GBP or USD. The risk premium appears in a first-order approximation of currency returns, $\Delta e_{t+1} = i_t + \rho_{t+1}$, which violates UIP. The related law of motion of the exchange rate is $e_t = \mathbf{E}_t e_{t+1} - \left(i_t + \mathbf{E}_t \rho_{t+1}\right)$, where $\mathbf{E}_t\{\cdot\}$ is the mathematical expectations operator conditional on date t information. Push the law of motion ahead a period, pass $\mathbf{E}_t\{\cdot\}$ through, replace $\mathbf{E}_t e_{t+1}$, and repeat $\mathcal{J}$ times to find

$$e_t = \mathbf{E}_t e_{t+J+1} - \sum_{j=0}^{\mathcal{J}} \mathbf{E}_t \left\{ i_{t+j} + \rho_{t+j+1} \right\}. \tag{1}$$

Equation (1) shows exchange rate fluctuations are driven by its expectation $\mathcal{J}$+1-periods ahead net of the sum of $\mathcal{J}$+1 expected returns that are excess, $\mathbf{E}_t \rho_{t+j}$, and otherwise, $\mathbf{E}_t i_{t+j}$.

3.b. Permanent and transitory components of the nominal exchange rate

Engel (2016) decomposes e_t into trend and transitory elements, $\tau_{e,t}$ and $\varepsilon_{e,t}$, using the Beveridge and Nelson (1981) decomposition and equation (1). The Beveridge-Nelson (BN) decomposition requires $\tau_{e,t}$ to be a random walk with drift, $\tau_{e,t} = \tau_e^* + \tau_{e,t-1} + \gamma_{e,\eta}\eta_{e,t}$, where $\eta_{e,t} \sim \mathcal{N}(0, 1)$. Taking $\mathcal{J} \to \infty$ in equation (1) yields

$$e_t = \tau_{e,t} - \sum_{j=0}^{\infty} \mathbf{E}_t \left\{ i_{t+j} + \rho_{t+1+j} \right\}, \tag{2}$$

where the BN trend is $\tau_{e,t} = \lim_{\mathcal{J}\to\infty} \mathbf{E}_t \left\{ e_{t+\mathcal{J}+1} - \mathcal{J}\tau_e^* \right\}$. Equation (2) decomposes e_t into $\tau_{e,t}$ and its transitory component, $\varepsilon_{e,t} = -\sum_{j=0}^{\infty} \mathbf{E}_t \left\{ i_{t+j} + \rho_{t+1+j} \right\}$, that restricts i_t and $\rho_t \sim I(0)$. Differencing equation (2) gives $\Delta e_t = \gamma_{e,\eta}\eta_{e,t} - \sum_{j=0}^{\infty} \mathbf{E}_t \left\{ i_{t+j} + \rho_{t+j+1} \right\} + \sum_{j=0}^{\infty} \mathbf{E}_{t-1} \left\{ i_{t+j-1} + \rho_{t+j} \right\}$. Following Nason and Rogers (2008), add and subtract $\mathbf{E}_{t-1} \left\{ i_{t+j} + \rho_{t+j+1} \right\}$ inside the brackets of the second infinite sum of the previous expression to obtain

$$\Delta e_t = -\left(i_{t-1} + \mathbf{E}_{t-1}\rho_t\right) + \sigma_{e,\eta}\eta_{e,t} + \left[\mathbf{E}_t - \mathbf{E}_{t-1}\right]\varepsilon_{e,t}. \tag{3}$$

Equation (3) connects excess currency returns to $\mathbf{E}_{t-1}\rho_t$, the innovation of $\tau_{e,t}$, and the forecast

innovation of $\varepsilon_{e,t}$, $\left[\mathbf{E}_t - \mathbf{E}_{t-1}\right]\varepsilon_{e,t} = -\sum_{j=0}^{\infty}\left[\mathbf{E}_t - \mathbf{E}_{t-1}\right]\left\{i_{t+j} + \rho_{t+1+j}\right\}$.

3.c A structural nominal currency return regression

We eliminate $\left[\mathbf{E}_t - \mathbf{E}_{t-1}\right]\varepsilon_{e,t}$ from equation (3) by assuming the joint probability distribution of y_t is a reduced-form VAR, $y_t = \sum_{\ell=1}^{k}\mathbf{B}_\ell y_{t-\ell} + \lambda_t$, where intercepts are ignored, $\mathbf{B}_\ell$ is a $n\times n$ matrix of lag coefficients, $n = 4$, $\left[\mathbf{I}_n - \mathbf{B}(\mathbf{L})\right]^{-1}$ is square summable, $\mathbf{B}(\mathbf{L}) = \sum_{\ell=1}^{k}\mathbf{B}_\ell\mathbf{L}^{\ell-1}$, and $\lambda_t \sim \mathcal{N}\left(\mathbf{0}_{n\times 1}, \boldsymbol{\Omega}_\lambda\right)$. A singularity in the VAR is ruled out by assuming p_t and the real exchange rate, $q_t \equiv e_t - p_t$, are $I(1)$, which implies e_t and p_t do not cointegrate. Stack k lags of y_t in $\mathcal{U}_t = \left[y_t' \;\; y_{t-1}' \;\; \ldots \;\; y_{t-k+1}'\right]'$ to construct the companion form of the reduced-form VAR, $\mathcal{U}_t = \boldsymbol{\mathcal{B}}\mathcal{U}_{t-1} + \Lambda_t$, where $\boldsymbol{\mathcal{B}}$ is the $nk\times nk$ companion matrix, $\Lambda_t = \left[\lambda_t' \;\; \mathbf{0}_{1\times n(n-1)}\right]'$ for $k > 1$, and $\Lambda_t = \lambda_t$ for $k = 1$. The companion form yields the j-month ahead forecast $\mathbf{E}_t\mathcal{U}_{t+j} = \boldsymbol{\mathcal{B}}^j\mathcal{U}_t$ and $\left(\mathbf{E}_t - \mathbf{E}_{t-1}\right)\mathcal{U}_{t+j} = \boldsymbol{\mathcal{B}}^j\Lambda_t$. Connecting this result to $\left[\mathbf{E}_t - \mathbf{E}_{t-1}\right]\varepsilon_{e,t}$ in equation (3) sets $\Delta e_t = -\left(i_{t-1} + \mathbf{E}_{t-1}\rho_t\right) + \gamma_{e,\eta}\eta_{e,t} - \left[s_i + s_\rho\boldsymbol{\mathcal{B}}\right]\left[\mathbf{I}_{n^2} - \boldsymbol{\mathcal{B}}\right]^{-1}\Lambda_t$, where s_i (s_ρ) is a $1\times nk$ vector full of zeros except for a one in the first (third) position. Using the companion form to eliminate $\mathbf{E}_{t-1}\rho_t = s_\rho\sum_{\ell=1}^{k}\mathbf{B}_\ell y_{t-\ell}$ and Λ_t in the last formula produces the regression

$$\Delta e_t = \alpha_{\Delta e,i}\, i_t + \alpha_{\Delta e,\pi}\,\pi_t + \alpha_{\Delta e,\rho}\,\rho_t + \sum_{\ell=1}^{k}\beta_\ell y_{t-\ell} + \gamma_{e,\eta}\eta_{e,t}, \tag{4}$$

where the impact and lag coefficients, $\alpha_{\Delta e,i}$, $\alpha_{\Delta e,\pi}$, $\alpha_{\Delta e,\rho}$, and $\beta_1, \ldots, \beta_k$, are nonlinear in $\boldsymbol{\mathcal{B}}$. Regression (4) restricts Δe_t. It responds to i_t, π_t, and ρ_t at impact, $\beta_1, \ldots, \beta_k$ drive persistence, and the innovation to $\tau_{e,t}$, $\eta_{e,t}$, scaled by $\gamma_{e,\eta}$ creates unsystematic variation in Δe_t.

3.d Identifying Exchange Rate-Risk Premium SVARs

The impact coefficients of regression (4) are short-run restrictions that help to identify the SVAR $\mathbf{A}y_t = \mathbf{A}\sum_{\ell=1}^{k}\mathbf{B}_\ell y_{t-\ell} + \boldsymbol{\Gamma}\,\eta_t$, where structural shocks have unit variances, $\eta_t \sim \mathcal{N}\left(\mathbf{0}_{n\times 1}, \mathbf{I}_n\right)$, the mapping from the structural to reduced-forms shocks is $\eta_t = \boldsymbol{\Gamma}^{-1}\mathbf{A}\,\lambda_t$, and $\boldsymbol{\Gamma}$ is a diagonal

matrix containing scale volatilities. We combine $a_{\Delta e,i}$, $a_{\Delta e,\pi}$, and $a_{\Delta e,\rho}$ with zeros imposed on the impact coefficients in the i_t, π_t, and ρ_t regressions to construct the impact matrix

$$\mathbf{A}_{\mathtt{BL}} = \begin{bmatrix} 1 & 0 & 0 & 0 \\ 0 & 1 & 0 & 0 \\ 0 & 0 & 1 & 0 \\ -a_{\Delta e,i} & -a_{\Delta e,\pi} & -a_{\Delta e,\rho} & 1 \end{bmatrix}, \tag{5}$$

of our baseline SVAR, SVAR-BL. Appendix A2 shows the restrictions imposed on $\mathbf{A}_{\mathtt{BL}}$ in equation (5) satisfy the necessary and sufficiency conditions for global identification of Rubio-Ramírez, Waggoner, and Zha (2010).

Relaxing three of the nine zero impact coefficients in the first three rows of $\mathbf{A}_{\mathtt{BL}}$ makes possible 510 impact matrices. We avoid analyzing all 510 by admitting into the model space only globally identified SVARs that order i_t first followed by π_t, ρ_t, and Δe_t and include $a_{\Delta e,i}$, $a_{\Delta e,\pi}$, and $a_{\Delta e,\rho}$. This shrinks the model space to SVAR-BL and 10 alternative globally identified SVARs with impact matrices $\mathbf{A}_{\mathtt{M1}}$, ..., $\mathbf{A}_{\mathtt{M9}}$, and $\mathbf{A}_{\mathtt{RC}}$, that are listed in table 1. Since $\mathbf{A}_{\mathtt{M1}}$, $\mathbf{A}_{\mathtt{M2}}$, $\mathbf{A}_{\mathtt{M3}}$, and $\mathbf{A}_{\mathtt{M4}}$ have at least one impact coefficient above the diagonal, the associated SVARs are non-recursive. Restrictions on $\mathbf{A}_{\mathtt{M5}}$ to $\mathbf{A}_{\mathtt{M9}}$ place at least one zero below the diagonal and zeros above the diagonal. There are no zeros below the diagonal of $\mathbf{A}_{\mathtt{RC}}$ giving SVAR-RC a recursive identification. The SVARs globally identify international financial, cross-country demand, risk premium, and trend exchange rate shocks.

4. The TVP-SV-SVAR and a MCMC Sampler

We introduce the TVP-SV-SVAR and outline the Metropolis in Gibbs MCMC sampler of Canova and Pérez Forero (2015) in this section.

4.a A TVP-SV-SVAR for the Chinese silver standard

Canova and Pérez Forero (2015) create a TVP-SV-SVAR(k) by endowing $\mathbf{A}$ and $\mathbf{B}_1 \ldots, \mathbf{B}_k$ of the fixed coefficient SVAR with TVPs and the scale volatilities of its diagonal matrix $\mathbf{\Gamma}$ with SVs

$$\mathbf{A}_t y_t = \mathbf{A}_t \mathbf{c}_t + \mathbf{A}_t \sum_{\ell=1}^{k} \mathbf{B}_{\ell,t} y_{t-\ell} + \mathbf{\Gamma}_t \eta_t, \quad \eta_t \sim \mathcal{N}\left(\mathbf{0}_{n\times 1}, \mathbf{I}_n\right), \tag{6}$$

where $\mathbf{c}_t$ is a $n\times 1$ vector of reduced-form TV intercepts.[7] The TVPs and SVs evolve as multivariate random walks with Gaussian innovations, $a_{t+1} = a_t + \psi_{t+1}$, $\psi_{t+1} \sim \mathcal{N}\left(\mathbf{0}, \mathbf{\Omega}_\psi\right)$, $\mathbb{B}_{t+1} = \mathbb{B}_t + \vartheta_{t+1}$, $\vartheta_{t+1} \sim \mathcal{N}\left(\mathbf{0}, \mathbf{\Omega}_\vartheta\right)$, and $\ln \gamma_{t+1}^2 = \ln \gamma_t^2 + \xi_{t+1}$, $\xi_{t+1} \sim \mathcal{N}\left(\mathbf{0}, \mathbf{\Omega}_\xi\right)$, where a_t is a vector of the off-diagonal TVPs of $\mathbf{A}_t$, $\mathbb{B}_t = \text{vec}\left(\left[\mathbf{B}_{1,t} \ \ldots \ \mathbf{B}_{k,t} \ \mathbf{c}_t\right]\right)$, and $\text{diag}\left(\mathbf{\Gamma}_t\right) \equiv \gamma_t = \left[\gamma_{1,t} \ \ldots \ \gamma_{n,t}\right]'$. Canova and Pérez Forero (CPF) assume a block diagonal covariance matrix

$$\mathcal{V} = \begin{bmatrix} \mathbf{I}_n & 0 & 0 & 0 \\ 0 & \mathbf{\Omega}_\vartheta & 0 & 0 \\ 0 & 0 & \mathbf{\Omega}_\psi & 0 \\ 0 & 0 & 0 & \mathbf{\Omega}_\xi \end{bmatrix}, \tag{7}$$

for the structural shocks, η_t, and random walk innovations ϑ_t, ψ_t, and ξ_t.

4.b A Metropolis in Gibbs MCMC sampler for TVP-SV-SVARs

Posterior distributions of the TVP-SV-SVARs of equation (6), the multivariate random walks of the TVPs and SVs, and equation (7) are assembled using the Metropolis in Gibbs MCMC sampler of CPF (2015). Their Metropolis in Gibbs MCMC sampler solves the problem of sampling from the posterior of a TVP-SV-SVAR that has a nonlinear likelihood induced by a non-recursive identification. This MCMC sampler is an algorithm organized around the correction to Primiceri (2005) devised by Del Negro and Primiceri (2015). The corrected sampler begins its dth iteration

[7] Implicit is the assumption that the elements of y_t are stationary. Appendix A1.6 reports Dickey-Fuller (DF) tests reject a unit root in i_t, π_t, ρ_t, and Δe_t on the China-U.K. and China-U.S. samples from 1912M04 to 1934M09. On the same samples, DF tests do not reject a unit root in p_t, e_t, and the real exchange rate, q_t.

with a Gibbs step to draw $\mathbb{B}_{1:T}$ using the Carter and Kohn (1994) multi-move scheme constrained by the Koop and Potter (2011) rule to toss out $\mathbb{B}_{1:T}$ if any $\mathbb{B}_t$ is explosive. Next, draw $a_{1:T}$ in a Metropolis step. Follow this with a Gibbs step grounded in the 10-point mixture normal distribution of Omori, Chib, Shephard, and Nakajima (2007) to draw $\gamma_{1:T}$. Iteration d finishes by drawing the covariance matrices, $\mathbf{\Omega}_\vartheta$, $\mathbf{\Omega}_\psi$, and $\mathbf{\Omega}_\xi$, in equation (7), where $d = 1, \ldots, \mathcal{D}$.

We take $\mathcal{D} = 500{,}000$ draws from posterior distributions of the TVP-SV-SVAR(k)s after $0.5\mathcal{D}$ burn-in steps, given the China-U.K. or China-U.S. sample, $y_{CUK,1:T}$ or $y_{CUS,1:T}$, our priors, and $k = 2$. Posterior distributions are thinned to $0.005\mathcal{D}$ by random sampling without replacement. Appendix A3 describes our priors and the CPF-Metropolis in Gibbs MCMC sampler.

5. Posterior Moments of the TVP-SV-SVARs

This section assesses the posterior distributions of the 11 TVP-SV-SVAR(2)s.

5.a. Evaluating the TVP-SV-SVARs on the China-U.K. and China-U.S. samples

We evaluate the TVP-SV-SVAR(2)s using marginal data densities (MDDs) and the widely applicable information criterion (WAIC) of Watanabe (2010). The MDDs are informative about which TVP-SV-SVAR(2) is preferred by $y_{CUK,1:T}$ or $y_{CUS,1:T}$. Geweke (2005) is our guide to computing the MDDs. The WAIC compliments the MDD by finding the TVP-SV-SVAR(2) that has the smallest posterior 1-month ahead predictive loss, given $y_{CUK,1:T}$ or $y_{CUS,1:T}$ and our priors. Gelman, et al (2014) advise calculating the WAIC as the negative of twice the posterior mean of the log predictive likelihood minus its variance. The variance of the posterior mean of the log predictive likelihood acts as a penalty term in the WAIC.

Table 2 has bold entries in the ln MDD and WAIC columns that indicate there is decisive evidence TVP-SV-SVAR(2)-`BL` offers the best fit and forecast (*i.e.*, largest ln MDD and smallest

WAIC) for $y_{CUK,1:T}$ and $y_{CUS,1:T}$. This is evidence the samples prefer the identification of the impact matrix of equation (5) that restricts i_t, π_t, and ρ_t to be causally prior to one another and to $\Delta e_{USD/S,t}$. Hence, the international financial shock affects $\Delta e_{GBP/S,t}$ $\left(\text{or } \Delta e_{USD/S,t}\right)$ at impact only through i_t. The same holds for the impact responses of currency returns to the π_t-cross-country demand shock and ρ_t-risk premium shock pairs. Since $y_{CUK,1:T}$ and $y_{CUS,1:T}$ prefer TVP-SV-SVAR(2)-BL, the rest of the paper focuses on its posterior distributions to study the Chinese silver standard.

5.b. Time-varying impact coefficients

Figure 2 displays moments of $a_{\Delta e,\,j,1:T,\,CUK}$ in the top row and $a_{\Delta e,\,j,1:T,\,CUS}$ in the bottom row taken from posterior distributions of TVP-SV-SVAR(2)-BL, $j = i$, π and ρ. Solid lines are posterior medians of the TVP-impact coefficients that are shaded by 68% Bayesian credible sets (*i.e.*, 16% and 84% quantiles).

Posterior medians of the impact coefficients exhibit co-movement with NBER recessions. The bottom row of figure 2 has posterior medians of $a_{\Delta e,i,1:T,\,CUS}$, $a_{\Delta e,\pi,1:T,\,CUS}$, and $a_{\Delta e,\rho,1:T,\,CUS}$ that peak and trough around every NBER recession from 1912M04 to 1934M09. Similarly, the top right panel of figure 2 shows peaks and troughs in the posterior medians of $a_{\Delta e,i,1:T,\,CUK}$ around five of these six NBER recessions with the 1926M10–1927M11 recession the exception. The same row reports peaks in the posterior medians of $a_{\Delta e,\pi,1:T,\,CUK}$ and $a_{\Delta e,\rho,1:T,\,CUK}$ during the 1929M08–1933M03 (*i.e.*, Great Depression) and 1920M01–1921M07 recessions.

The co-movement displayed in figure 2 points to mean reversion in the posterior medians of the impact coefficients. Mean reversion is evident in the posterior medians of $a_{\Delta e,\pi,1:T,\,CUS}$ that fluctuate around one in the lower middle panel of the figure. The 68% Bayesian credible sets in the panel cover one in 190 of the 270 months of the sample suggesting an approximation

of relative purchasing power parity (PPP) held for $\Delta e_{USD/S,t}$ and $\pi_{S,t} - \pi_{US,t}$ under the Chinese silver standard. Posterior medians of $a_{\Delta e,\rho 1:T,CUS}$ wander around zero in the lower right panel of figure 2 showing parity was restored to the Chinese silver standard at the same frequency as the six NBER recessions of the sample. The bottom left panel of figure 2 depicts mean reversion in posterior medians of $a_{\Delta e,i,1:T,CUS}$, which are always negative. Since $i_{S,t} > i_{US,t}$ produced an appreciation in the Shanghai *tael*, it carried less risk than the USD.

Figure 2 presents dissimilar posterior distributions of $a_{\Delta e,i,1:T,CUK}$, $a_{\Delta e,\pi,1:T,CUK}$, and $a_{\Delta e,\rho,1:T,CUK}$. First, posterior medians of $a_{\Delta e,i,1:T,CUK} > 0$ in the top left panel. Hence, $e_{GBP/S,t}$ depreciated in response to $i_{S,t} > i_{UK,t}$ making the Shanghai *tael* riskier than the GBP. Second, claims to relative PPP holding are weakened for $\Delta e_{GBP/S,t}$ and $\pi_{S,t} - \pi_{UK,t}$ in the top middle panel because, although posterior medians of $a_{\Delta e,\pi,1:T,CUK}$ move around one, these moments and the associated 68% Bayesian credible sets vary more compared with the panel below. Lastly, the top right panel shows posterior medians of $a_{\Delta e,\rho,1:T,CUK}$ predict a one percent change in ρ_t generated a 40 to 60 basis point increase in $e_{GBP/S,t}$. These responses contrast with the mean reversion returning $e_{USD/S,t}$ to parity observed in the bottom right panel of figure 2.

5.c. The Chinese silver standard: Volatility

Figure 3 depicts posterior medians of the SVs with solid lines that are covered by 68% Bayesian credible sets. These moments of the posterior distributions of TVP-SV-SVAR-BL are conditional on $y_{CUK,1:T}$ $\left(y_{CUS,1:T}\right)$ in the top (bottom) row of figure 3. From left to right, its columns contain posterior moments of $\gamma_{i,1:T,j}$, $\gamma_{\pi,1:T,j}$, $\gamma_{\rho,1:T,j}$, and $\gamma_{\Delta e,1:T,}$, $j = CUK, CUS$.

Seven of eight posterior median SVs peak during NBER recessions in figure 3. Five peak in the 1920M01–1921M07 recession $\left(\gamma_{\pi,1:T,CUK}, \gamma_{\rho,1:T,CUK}, \gamma_{\Delta e,1:T,CUK}, \gamma_{i,1:T,CUS}, \gamma_{\pi,1:T,CUS},\right)$. Peaks in posterior medians of $\gamma_{\rho,1:T,CUS}$ and $\gamma_{\Delta e,1:T,CUS}$ coincide with the 1918M08–1919M03

recession and Great Depression, respectively. The exception is the peak in posterior medians of $\gamma_{i,1:T,CUK}$ at 1921M10. Posterior median SVs have secondary peaks in the First World War $\left(\gamma_{\pi,t,CUS}$ and $\gamma_{\Delta e,t,CUS}\right)$, the 1918M08–1919M03 $\left(\gamma_{\Delta e,t,CUK}\right)$, 1923M05–1924M07 $\left(\gamma_{i,t,CUK}$ and $\gamma_{i,t,CUS}\right)$, and 1926M10–1927M11 $\left(\gamma_{\rho,t,CUK}$ and $\gamma_{\rho,1:T,CUS}\right)$ recessions, and Great Depression $\left(\gamma_{\pi,t,CUK}\right)$. No peaks match the U.S. Silver Purchase Act of 1934M06.

Figure 3 also shows posterior medians of the SVs are falling at the end of the sample except for $\gamma_{\rho,1:T,CUK}$ and $\gamma_{\rho,1:T,CUS}$. These medians take a W-shaped path from a peak in 1920M06 and 1918M09 to 1934M09, but substantial disparities exist in the height of these peak SVs compared with observations from 1934M06 to 1934M09. Posterior medians during these months are 50 to 60% less than the peaks of $\gamma_{\rho,1:T,CUK}$ at 1920M06 and $\gamma_{\rho,1:T,CUS}$ at 1918M09.

6. Time-varying UIP, Predictability, and (In)Stability

This section employs monthly tests of UIP, predictability and instability statistics, and IRFs to study the efficiency and (in)stability of the Chinese silver standard.

6.a The Chinese silver standard; Time-varying tests of UIP

Rejections of UIP on the Chinese silver standard are only on the China-U.K. sample from spring 1918 into the 1920s. The evidence is obtained by adapting methods of Hodrick (1992) to test the Chinese silver standard for violations of UIP. We use his formulas and posterior distribution of a TVP-SV-SVAR to compute the TV-slope coefficient, δ_t, of the Fama regression proposed by Engel (2016) that runs $\Delta e_{t+1} + \left(i_{j,t} - i_{S,t}\right)$ on a constant and $i_{j,t} - i_{S,t}$ and its real exchange rate cousin that regresses $\Delta q_{t+1} + \left(r_{j,t} - r_{S,t}\right)$ on a constant and $r_{j,t} - r_{S,t}$ yielding the TV-slope coefficient ϱ_t, where the ex ante real rate spread $r_t = i_t - \mathbf{E}_t \pi_{t+1}$, $r_t = r_{S,t} - r_{j,t}$, and $j = UK, US$. The null hypotheses of UIP are $\delta_t = 1$ and $\varrho_t = 1$ at $t = 1, \ldots, T$.

Engel (2016) stresses the signs of $\text{cov}\left(\mathbf{E}_t \rho_{t+1},\, r_{j,t} - r_{S,t}\right)$ and $\text{cov}\left(\mathbf{E}_t \sum_{j=0}^{\infty} \rho_{t+j+1},\, r_{j,t} - r_{S,t}\right)$ are useful for studying UIP. Rejection rests on either covariance not equaling zero, but the $\text{cov}\left(\mathbf{E}_t \rho_{t+1},\, r_{j,t} - r_{S,t}\right) > 0$ and $\text{cov}\left(\mathbf{E}_t \sum_{j=0}^{\infty} \rho_{t+j+1},\, r_{j,t} - r_{S,t}\right) < 0$ summarize Engel's exchange rate-risk premium paradox. The first inequality signals there is excess sensitivity of Δe_{t+1} to a change in i_t. This points to greater risk on the Shanghai *tael* compared with the *GBP* or *USD*. The latter inequality is about excess volatility in e_t that implies a stronger Shanghai *tael* carried less risk. Appendix A4 shows the TV-slope coefficient, $\phi_{H,t}$, of the long-horizon regression $\rho_{t+1} = \phi_{0,t} + \phi_{H,t} \sum_{h=0}^{H-1} \left(r_{j,t-h} - r_{S,t-h}\right) + \zeta_{\rho,t+1}$ approximates the sign of $\text{cov}_t \left(\mathbf{E}_t \sum_{j=0}^{\infty} \rho_{t+j+1},\, r_{j,t} - r_{S,t}\right)$ and replicates it as $H \to \infty$. The sign of $\text{cov}_t \left(\mathbf{E}_t \rho_{t+1},\, r_{j,t} - r_{S,t}\right)$ is recovered from $\phi_{H,t}$ when $H = 1$. We use formulas in Hodrick (1992), which are also described in Appendix A4, to compute $\phi_{h,t}$, $h = 1, \ldots, H$, given a TVP-SV-SVAR.

Figure 4 collects posterior moments of $\delta_{1:T,\,j}$, $\varrho_{1:T,\,j}$, $\phi_{1,1:T,\,j}$, and $\phi_{3,1:T,\,j}$ for $j = CUK$ in the top and $j = CUS$ in the bottom row in panels from left to right. The posterior distributions of TVP-SV-SVAR(2)-BL conditional on $y_{1:T,CUK}$ $\left(y_{1:T,CUS}\right)$ and our priors yield medians (solid lines) shaded by 68% Bayesian credible sets in the top (lower) row of figure 4. Since posterior medians of $\phi_{H,1:T} \approx 0$ at $H > 3$, we report long-horizon regressions at $H = 3$.

Rejections of UIP appear in the upper middle two panels of figure 4 that display posterior moments of $\varrho_{1:T,\,CUK}$ and $\phi_{1,1:T,CUK}$. The 68% Bayesian credible sets of $\varrho_{1918\text{M}12:1920\text{M}06,\,CUK}$ exclude one. These dates run from the month after the First World War ceased to two months after the Bank of England rate hit 7%, which Howson (1974) argues ended the U.K.'s post-war boom. More evidence against UIP are 68% Bayesian credible sets of $\phi_{1,1918\text{M}07:1927\text{M}11,\,CUK}$ that are bounded above zero. At the 1-month horizon, investors anticipated excess returns on deposits in *GBP* compared with Shanghai *tael* from two months after a new Governor began at

the Bank of England to the trough of the 1926M10–1927M11 recession.

The other six panels of figure 4 lack evidence to reject UIP. The 68% Bayesian credible sets of $\delta_{1:T,CUK}$ $\left(\phi_{3,1:T,CUK}\right)$ always cover one (zero) in the top row of figure 4. Its bottom row shows UIP is not rejected on $e_{USD/S,t}$ because one (zero) is in the 68% Bayesian credible sets of $\delta_{1:T,CUS}$ and $\varrho_{1:T,CUS}$ $\left(\phi_{1,1:T,CUS}\text{, and } \phi_{3,1:T,CUS}\right)$. However, $e_{GBP/S,t}$ often satisfies the exchange rate-risk premium paradox of Engel (2016). The posterior medians of $\phi_{1,1:T,CUK} > 0$ and $\phi_{3,1917M03:T,CUK} < 0$ in the last two panels of the top row of figure 4. In its bottom row, signs of the posterior medians of $\phi_{1,1:T,CUS}$ and $\phi_{3,1:T,CUS}$ are reversed for $e_{USD/S,t}$.

6.b. The Chinese Silver Standard: Predictability of deviations from trend of p_t and e_t

Cogley, Primiceri, and Sargent (2010) propose a h-step ahead TV predictability statistic, $\mathcal{R}^2_{z,h,t}$, for $z_t \sim I(1)$ that is one minus the ratio of its conditional to its unconditional variance. We follow them invoking the anticipated utility model (AUM) of Kreps (1998) to address the problem of forecasting with TVPs and SVs, which makes $\mathcal{R}^2_{z,h,t}$ an approximation. Nevertheless, $\mathcal{R}^2_{z,h,t}$ reports on the h-month ahead predictability of deviations from trend of z_t. If z_t is unpredictable, $\mathcal{R}^2_{z,h,t} = 0$ for all h and dates t. Furthermore, $\lim_{h\to\infty} \mathcal{R}^2_{z,h,t} = 0$. Predictability places $\mathcal{R}^2_{z,h,t} \in [0, 1)$, which when rising is evidence of decreasing stability in z_t at the h-month ahead horizon. Appendix A6 reviews our calculation of $\mathcal{R}^2_{z,h,t}$ using a TVP-SV-SVAR.

Figure 5 plots posterior medians (solid lines) and 68% Bayesian credible sets of $\mathcal{R}^2_{p,1,1:T}$, $\mathcal{R}^2_{p,6,1:T}$, $\mathcal{R}^2_{e,1,1:T}$ and $\mathcal{R}^2_{e,6,1:T}$ from 1912M04 to 1934M09 in columns from left to right. The top (bottom) row displays moments taken from the posterior distribution of TVP-SV-SVAR(2)-BL conditional on $y_{1:T,CUK}$ $\left(y_{1:T,CUS}\right)$ and our priors.

The best predictability of deviations from trend is in the left column of figure 5. Its top and bottom panels display posterior medians of $\mathcal{R}^2_{p,1,1:T} > \mathcal{R}^2_{p,6,1:T}$, $\mathcal{R}^2_{e,1,1:T}$, and $\mathcal{R}^2_{e,6,1:T}$ in the

rest of the figure. Comparing posterior medians of $\mathcal{R}^2_{p,1,t}$ shows the top left panel offers more (less) predictability values from 1912M04 to 1920M07 (1920M08 to 1934M09). The same top (bottom) panel also shows posterior medians of $\mathcal{R}^2_{p,1,t}$ increasing from 1932M09 (1927M01) to 1934M09. The start date coincides with the month the Nanjing government ended the fourth encirclement campaign of the Eyuwan Soviet (obtained control of the Shanghai Customs Office), which is two (more than seven) years before the U.S. Silver Purchase Act of 1934M06.

The last three columns of figure 5 display posterior moments of $\mathcal{R}^2_{p,6,1:T}$, $\mathcal{R}^2_{e,1,1:T}$, and $\mathcal{R}^2_{e,6,1:T}$. The 68% Bayesian credible sets of $\mathcal{R}^2_{p,6,t}$ are well above zero by no later than the end of the First World War in the second column of panels, but at the 1-month horizon the third column shows predictability of deviations from trend for $e_{GBP/S,t}$ and $e_{USD/S,t}$ from 1912M04 to 1934M09. However, the right top and bottom panels of figure 5 display 68% Bayesian credible sets with lower quantiles ranging from zero to 0.008. Hence, predictability of deviations from trend for $e_{GBP/S,1:T}$ and $e_{USD/S,1:T}$ is vanishing by the 6-month horizon.

6.c. The Chinese Silver Standard: (In)Stability of p_t and e_t

We gauge instability in the Chinese silver standard with a statistic developed by Cogley and Sargent (2015). They calculate instability in the $I(1)$ variable z_t as the square root of the sum of two components. The first is the forward-looking uncertainty around $\mathbf{E}_t \Delta z_{t+h}$, which is the conditional variance of this forecast, $\mathcal{V}_t\left(z_{t+h} - \mathbf{E}_t z_{t+h}\right)$. Add to this the variance of the h-month ahead expected accumulated growth of z_t, $\mathbf{E}_t z_{t+h} - z_t$. The result is the Cogley and Sargent measure of instability $\sigma_{z,h,t} \approx \sqrt{\mathcal{V}_t\left(z_{t+h} - \mathbf{E}_t z_{t+h}\right) + \left(\mathbf{E}_t z_{t+h} - z_t\right)^2}$; see their equation (8). We appeal to the AUM, as in Cogley and Sargent (2015), to compute $\sigma_{z,h,t}$ on the posterior distributions of TVP-SV-SVAR(2)-BL. Appendix A7 has details about adapting Cogley and Sargent (2015) to calculate $\sigma_{z,h,t}$ on a TVP-SV-SVAR.

Figure 6 displays posterior distributions of $\sigma_{p,h,1:T}$ and $\sigma_{e,h,1:T}$ at 1- and 12-month horizons in columns from left to right on the 1912M04–1934M09 sample. The 68% Bayesian credible sets cover solid lines that are posterior medians. Distributions in the top (bottom) row depend on TVP-SV-SVAR(2)-BL, $y_{CUK,1:T}$ $\left(y_{CUS,1:T}\right)$ and our priors.

The Chinese silver standard saw instability peak during the 1920M01–1921M07 recession and Great Depression as shown in the top and bottom rows of figure 6. In the top row, posterior medians of $\sigma_{p,1,t}$, $\sigma_{p,12,t}$, $\sigma_{e,1,t}$, and $\sigma_{e,12,t}$ peak at 1921M02, 1920M11, 1920M12, and 1920M12, respectively. The same row has secondary peaks in the posterior medians of these instability statistics in 1931M10 remembering the U.K. left the gold standard and Japan invaded Manchuria the previous month. In contrast, the bottom row of figure 6 shows posterior medians of $\sigma_{p,1,t}$, $\sigma_{p,12,t}$, $\sigma_{e,1,t}$, and $\sigma_{e,12,t}$ peaking during the 1920M01–1921M07 recession and the Great Depression at 1920M10, 1931M05, 1931M05, and 1931M06. The secondary peaks occur at 1931M05, 1920M10, 1920M04, and 1920M04 in the same row of the figure.

Posterior distributions of $\sigma_{p,1,t}$, $\sigma_{p,12,t}$, $\sigma_{e,1,t}$, and $\sigma_{e,12,t}$ shift down after the Great Depression in figure 6. The upshot is that, although 68% Bayesian credible sets are wider around posterior medians at the 12-month horizon in 1933 and 1934, figure 6 shows the posterior medians are lower after the Great Depression.

6.d. The Chinese Silver Standard: TV-IRFs in 1934

Figure 7 (8) reports posterior median IRFs at 1934M01, 1934M06, and 1934M09 created using the TVP-SV-SVAR(2)-BL conditional on $y_{1:T,CUK}$ $\left(y_{1:T,CUS}\right)$ and our priors. The dates are six months before the U.S. Silver Purchase Act became law, its month of passage, and end of the sample. The top row depicts IRFs of i_t with respect to international financial, cross-country demand, risk premium, and trend exchange rate shocks from impact to the 12-month horizon.

The IRFs of p_t, ρ_t, and e_t on the same shocks appear in the next three rows in figures 7 and 8. We accumulate IRFs of π_t and Δe_t to compute IRFs of p_t and e_t.

The structural shocks produce median posterior IRFs of i_t and ρ_t at 1934M01, 1934M06, and 1934M09 in figures 7 and 8 that are mean reverting. The top row of figures 7 and 8 have posterior median IRFs of i_t that return to steady state by five months after an international financial, a cross-country demand, a risk premium, or a trend exchange rate shock. The four shocks also produce posterior median IRFs of ρ_t in figures 7 and 8 that revert to steady state by the 5-month horizon. This shows equilibrium was restored to the Chinese silver standard in less than half a year after a shock to parity during 1934.

The four shocks produce posterior median IRFs of p_t and e_t at 1934M01, 1934M06, and 1934M09 in figures 7 and 8 that often predict $p_{S,t}$ increasing faster than either $p_{UK,t}$ or $p_{US,t}$ and depreciation of $e_{GBP/S,T}$ and $e_{USD/S,T}$. The depreciation predicted for the Shanghai *tael* is found in the positive hump-shaped posterior median IRFs to the cross-country demand, risk premium, and trend exchange rate shocks in the bottom row of the figures. The international financial shock also produces hump-shaped posterior median IRFs of e_t in the bottom left panels of figures 7 and 8. However, the latter panel shows these IRFs are always less than zero, which indicates the international financial shock generated an appreciation of $e_{USD/S,T}$.

Lastly, we garner evidence about the stability of the Chinese silver standard from 1934M01 to 1934M09 by comparing posterior median IRFs in figure 7 and figure 8. Going panel by panel finds the posterior median IRFs at 1934M01, 1934M06, and 1934M09 are often identical in height, shape, and persistence. Hence, figures 7 and 8 give additional evidence the U.S. Silver Purchase Act of 1934M06 had little impact on the Chinese silver standard before it was broken by the Nanjing government in 1934M10.

7. Conclusion

This paper reexamines the debate about the end of the Chinese silver standard. The question is whether the Chinese silver standard failed because its operating mechanism was fragile or the U.S. Silver Purchase Act of 1934M06 drained China of silver. The hypotheses are assessed using structural VARs (SVARs) that include time varying parameters (TVPs) and stochastic volatility (SV) on China-U.K. and China-U.S. samples from 1912M04 to 1934M09.

We estimate 11 TVP-SV-SVARs with Bayesian methods. The results show the Chinese silver standard weathered episodes of instability during the 1920M01–1921M07 recession and Great Depression. Rising predictability in deviations from trend of the China-U.K. and China-U.S. WPI differentials begins two years or more before the U.S. Silver Purchase Act of 1934M06. Impulse response functions that are nearly identical moving variable by variable and shock by shock in 1934M01, 1934M06, and 1934M09 provide more testimony this act of the U.S. Congress had little impact on the Chinese silver standard. We conclude the Chinese silver standard did not collapse because of its own fragility or the actions of the U.S. Congress.

This leaves actions the Nanjing government took starting in 1934M10 to explain the demise of the Chinese silver standard. Brandt and Sargent (1989) argue the Chinese silver standard was disrupted by the Nanjing government pursuing goals that caused private agents to revise their expectations about the future of money in China. After 1934M10, changes in these expectations lead to a growing exodus of silver from China that, according to Brandt and Sargent, contributed to the Nanjing government replacing the Chinese silver standard with the *fabi* in 1935M11. We hope this paper encourages research on the Chinese silver standard and the consequences of policy making that is at odds with private sector expectations.

References

Beveridge, S., C.R. Nelson (1981). A new approach to decomposition of economic time series into permanent and transitory components with particular attention to measurement of the business cycle. *Journal of Monetary Economics* 7, 151–174.

Brandt, L., D. Ma, T.G. Rawski (2014). From divergence to convergence: Reevaluating the history behind China's economic boom. *Journal of Economic Literature* 52, 45–123.

Brandt, L., T.J. Sargent (1989). Interpreting new evidence about China and U.S. silver purchases. *Journal of Monetary Economics* 23, 31–51.

Bratter, H.M. (1933). The monetary use of silver in 1933. Trade Promotion Series, No. 149, Department of Commerce. Washington, D.C.: U.S. Government Printing Office.

Burdekin, R.C.K. (2008). US pressure on China: Silver flows, deflation, and the 1934 Shanghai credit crunch. *China Economic Review* 19, 170–182.

Canova, F., F.J. Pérez Forero (2015). Estimating overidentified, non-recursive, time varying coefficient structural VARs. *Quantitative Economics* 6, 359–384.

Carter, C.K., R. Kohn (1994). On Gibbs sampling for state space models. *Biometrika* 81, 541–553.

Chang, P-H.K. (1988). Commodity price shocks and international finance. Unpublished dissertation, Department of Economics, MIT, Cambridge, MA.

Chen, B., D. Li, Y. Xie (2022). Silver, fiduciary money, and the Chinese economy, 1890–1935. *Review of International Economics* 30, 939–970.

Cogley, T., G.E. Primiceri, T.J. Sargent (2010). Inflation-gap persistence in the US. *American Economic Journal: Macroeconomics* 2, 43–69.

Cogley, T., T.J. Sargent (2015). Measuring price-level uncertainty and instability in the United States, 1850–2012. *Review of Economics & Statistics* 97, 827–838.

Dean, A. (2020). China and the End of Global Silver, 1873–1937. Ithaca, NY: Cornell University Press.

Del Negro, M., G.E. Primiceri (2015). Time varying structural vector autoregressions and monetary policy: A corrigendum. *Review of Economic Studies* 82, 1342–1345.

Engel, C. (2016). Exchange rates, interest rates, and the risk premium. *American Economic Review* 106, 436–474.

Friedman, M. (1992). Franklin D. Roosevelt, silver and China. *Journal of Political Economy* 100, 62–83.

Friedman, M., A.J. Schwartz (1963). A Monetary History of the United States, 1867–1960. Princeton, NJ: Princeton University Press.

Gelman, A., J.B. Carlin, H.S. Stern, D.B. Dunsun, A. Vehtari, D.B. Rubin (2014). Bayesian Data Analysis, 3rd edition. New York, NY: CRC Press, Taylor & Francis Group.

Geweke, J. (2005). Contemporary Bayesian Econometrics and Statistics. New York, NY: J. Wiley & Sons.

Ho, C-Y., D. Li (2014). A mirror of history: China's bond market, 1921–42. *Economic History Review* 67, 409–434.

Ho, T-K. (2014). Dilemma of the silver standard economies: The case of China. *Southern Economic Journal* 81, 519–534.

Ho, T-K., C-C. Lai (2013). Silver fetters? The rise and fall of the Chinese price level 1928–34. *Explorations in Economic History* 50, 446–462.

Ho, T-K., C-C. Lai (2016). A silver lifeboat, not silver fetters: Why and how the silver standard insulated China from the Great Depression. *Journal of Applied Econometrics* 32, 403–419.

Ho, T-K., C-C. Lai, J.J-S. Gau (2013). Equilibrium and adjustment of exchange rates in the Chinese silver standard economy, 1928–1935. *Cliometrica* 7, 87–98.

Hodrick, R.J. (1992). Dividend yields and expected stock returns: Alternative procedures for inference and measurement. *Review of Financial Studies* 5, 357–386.

Howson, S. (1974). The origins of dear money, 1919–20. *Economic History Review*, 27, 88–107.

Jacks, D.S., S. Yan, L. Zhao. (2017). Silver points, silver flows, and the measure of Chinese financial integration. *Journal of International Economics* 108, 377–386.

Kong, M. (1988). Nankai Jingji Zhishu Ziliao Huibian (Nankai Collection: Economic Index Materials). Beijing, China: Social Sciences Press.

Koop, G., S. Potter (2011). Time varying VARs with inequality restrictions. *Journal of Economic Dynamics & Control* 35, 1126–1138.

Kreps, D. (1998). Anticipated utility and dynamic choice. In Frontiers of Research in Economic Theory: The Nancy L. Schwartz Memorial Lectures, 1983–1997. Jacobs, D.P., E. Kalai, M.I. Kamien, N.L. Schwartz (eds.), Cambridge, UK: Cambridge University Press.

Lai, C-C., J.J-S. Gau (2003). The Chinese silver standard economy and the 1929 Great Depression. *Australian Economic History Review* 43, 155–168.

Leavens, D.H. (1939). Silver Money. Cowles Commission for Research in Economics, Monograph no. 4. Bloomington, IN: Principia Press, Inc.

Ma, D. (2019). Financial revolution in Republican China during 1900–37: A survey and a new interpretation. *Australian Economic History Review* 59, 242–262.

Ma, D., L. Zhao (2020). A silver transformation: Chinese monetary integration in times of political disintegration, 1898–1933. *Economic History Review*, 73, 513–539.

Nason, J.M., J.H. Rogers. (2008). Exchange rates and fundamentals: A generalization. Working paper 2008–16, Federal Reserve Bank of Atlanta.

Omori, Y., S. Chib, N. Shephard, J. Nakajima (2007). Stochastic volatility with leverage: Fast and efficient likelihood inference. *Journal of Econometrics* 140, 425–449.

Palma, N., L. Zhao (2021). The efficiency of the Chinese silver standard, 1920–1933. *Journal of Economic History* 81, 872–908.

Primiceri, G.E. (2005). Time varying structural vector autoregressions and monetary policy. *Review of Economic Studies* 72, 821–852.

Rawski, T. (1993). Milton Friedman, silver and China. *Journal of Political Economy* 101, 755–758.

Rubio-Ramírez, J.F., D.F. Waggoner, T. Zha (2010). Structural vector autoregressions: Theory of identification and algorithms for inference. *Review of Economic Studies* 77, 665–696.

Shanghai Research Institute of Economics, Chinese Academy of Sciences and Research Institute of Economics, Shanghai Social Sciences Academy (1958). *Shanghai chieh-fang chien-hou we-chia tzu-liao hui-pien* (A Collection of Data on Prices in Shanghai before and after Liberation), 1921–1957. Shanghai, China: Shanghai People's Publishing House.

Shiroyama, T. (2008). China During the Great Depression: Market, State, and the World Economy, 1929–1937. Cambridge, MA: Harvard University Asia Center.

Silber, W.L. (2019). The Story of Silver: How the White Metal Shaped America and the Modern World. Princeton, NJ: Princeton University Press.

Young, J.P. (1931). The Shanghai tael. *American Economic Review* 21, 682–684.

Watanabe, S. (2010). Asymptotic equivalence of Bayes cross validation and widely applicable information criterion in singular learning theory. *Journal of Machine Learning Research* 11, 3571–3594.

Wu, D. (1935). Yige xinde waihui zhishu (A new exchange rate index). *Review of Political Economy* 21, 463–509.

Zhao, L., Y. Zhao (2018). Alfred Marshall, Silver, and China. *Australian Economic History Review* 58, 153–175.

Zhongguo ren min yin hang Shanghai Shi fen hang (People's Bank of China, Shanghai Branch) (1960). *Shanghai qianzhuang shiliao* (Shanghai Banking Historical Records). Shanghai People's Press: Shanghai, China.

Table 1. Impact Matrices of the Alternative Globally Identified SVARs

$$\mathbf{A}_{\mathtt{M1}} = \begin{bmatrix} 1 & 0 & 0 & 0 \\ 0 & 1 & 0 & -a_{\pi,\Delta e} \\ 0 & 0 & 1 & -a_{\rho,\Delta e} \\ -a_{\Delta e,i} & -a_{\Delta e,\pi} & -a_{\Delta e,\rho} & 1 \end{bmatrix} \quad \mathbf{A}_{\mathtt{M2}} = \begin{bmatrix} 1 & 0 & 0 & 0 \\ 0 & 1 & -a_{\pi,\rho} & 0 \\ 0 & 0 & 1 & -a_{\rho,\Delta e} \\ -a_{\Delta e,i} & -a_{\Delta e,\pi} & -a_{\Delta e,\rho} & 1 \end{bmatrix}$$

$$\mathbf{A}_{\mathtt{M3}} = \begin{bmatrix} 1 & 0 & 0 & 0 \\ 0 & 1 & 0 & -a_{\pi,\Delta e} \\ 0 & -a_{\rho,\pi} & 1 & 0 \\ -a_{\Delta e,i} & -a_{\Delta e,\pi} & -a_{\Delta e,\rho} & 1 \end{bmatrix} \quad \mathbf{A}_{\mathtt{M4}} = \begin{bmatrix} 1 & 0 & 0 & 0 \\ 0 & 1 & -a_{\pi,\rho} & 0 \\ -a_{\rho,i} & 0 & 1 & 0 \\ -a_{\Delta e,i} & -a_{\Delta e,\pi} & -a_{\Delta e,\rho} & 1 \end{bmatrix}$$

$$\mathbf{A}_{\mathtt{M5}} = \begin{bmatrix} 1 & 0 & 0 & 0 \\ 0 & 1 & 0 & 0 \\ 0 & -a_{\rho,\pi} & 1 & 0 \\ -a_{\Delta e,i} & -a_{\Delta e,\pi} & -a_{\Delta e,\rho} & 1 \end{bmatrix} \quad \mathbf{A}_{\mathtt{M6}} = \begin{bmatrix} 1 & 0 & 0 & 0 \\ 0 & 1 & 0 & 0 \\ -a_{\rho,i} & 0 & 1 & 0 \\ -a_{\Delta e,i} & -a_{\Delta e,\pi} & -a_{\Delta e,\rho} & 1 \end{bmatrix}$$

$$\mathbf{A}_{\mathtt{M7}} = \begin{bmatrix} 1 & 0 & 0 & 0 \\ -a_{\pi,i} & 1 & 0 & 0 \\ 0 & 0 & 1 & 0 \\ -a_{\Delta e,i} & -a_{\Delta e,\pi} & -a_{\Delta e,\rho} & 1 \end{bmatrix} \quad \mathbf{A}_{\mathtt{M8}} = \begin{bmatrix} 1 & 0 & 0 & 0 \\ 0 & 1 & 0 & 0 \\ -a_{\rho,i} & -a_{\rho,\pi} & 1 & 0 \\ -a_{\Delta e,i} & -a_{\Delta e,\pi} & -a_{\Delta e,\rho} & 1 \end{bmatrix}$$

$$\mathbf{A}_{\mathtt{M9}} = \begin{bmatrix} 1 & 0 & 0 & 0 \\ -a_{\pi,i} & 1 & 0 & 0 \\ 0 & -a_{\rho,\pi} & 1 & 0 \\ -a_{\Delta e,i} & -a_{\Delta e,\pi} & -a_{\Delta e,\rho} & 1 \end{bmatrix} \quad \mathbf{A}_{\mathtt{RC}} = \begin{bmatrix} 1 & 0 & 0 & 0 \\ -a_{\pi,i} & 1 & 0 & 0 \\ -a_{\rho,i} & -a_{\rho,\pi} & 1 & 0 \\ -a_{\Delta e,i} & -a_{\Delta e,\pi} & -a_{\Delta e,\rho} & 1 \end{bmatrix}$$

Notes: Global identification is verified using criteria developed by Rubio-Ramírez, Waggoner, and Zha (2010). The (d, j) element of $\mathbf{A}_\ell$ is the impact coefficient a_{dj}, where $d \neq j$ and $\ell = \mathtt{M1}, \ldots, \mathtt{M9}$, and $\mathtt{RC}$, where $\mathtt{Mx}$ denotes SVAR $\mathtt{x} = 1, \ldots, 9$, and $\mathtt{RC}$ is the recursive SVAR. Equation (5) has the impact matrix of our baseline SVAR, SVAR-$\mathtt{BL}$.

Table 2. MDDs and WAICs of the Baseline and Alternative Globally Identified SVARs on the China-U.K. and China-U.S. Samples, 1912M04–1934M09

	$y_{CUK,1:T}$		$y_{CUS,1:T}$	
SVAR	ln MDD	WAIC	ln MDD	WAIC
BL	**−2049.45**	**5838.59**	**−2115.40**	**5853.55**
M1	−2564.19	6150.10	−2826.01	6067.70
M2	−2508.43	6088.25	−2716.09	6180.55
M3	−2151.04	5985.73	−2331.61	5941.21
M4	−2247.96	5908.49	−2426.98	5923.75
M5	−2257.41	5847.40	−2244.37	5889.24
M6	−2185.39	5905.78	−2170.32	5883.31
M7	−2173.85	5840.45	−2363.15	5940.85
M8	−2167.46	5867.85	−2221.30	5868.09
M9	−2249.30	5858.85	−2224.19	5876.26
RC	−2421.83	5967.97	−2542.05	6007.94

Notes: Log marginal data densities (MDDs) appear in the column headed lnMDD. The MDDs are calculated using the harmonic mean estimator of Geweke (2005), 2,500 draws from the posterior of the TVP-SV-SVAR(2)s, the China-U.K. and China-U.S samples, $y_{CUK,1:T}$ and $y_{CUS,1:T}$, and our priors. The support $y_{CUK,1:T}$ or $y_{CUS,1:T}$ give to a TVP-SV-VAR(2) is summarized by its MDD. The column headed WAIC reports the widely applicable information criterion of Watanabe (2010), which is also known as the Watanabe-Akaike-IC. The WAIC is an estimate of the 1-month ahead predictive loss of a TVP-SV-SVAR(2). Gelman et al (2014) advise computing the predictive loss as twice the difference between a penalty term and the mean of the log predictive likelihoods. Estimates of the likelihood are obtained from the predictive steps of the Kalman filter and posterior of a TVP-SV-SVAR(2). The penalty term of the WAIC measures the effective dimension of the parameter vector. It is the sum of the posterior variances of the likelihood of a TVP-SV-SVAR(2). Values in bold are the largest ln MDD and smallest WAIC on $y_{CUK,1:T}$ or $y_{CUS,1:T}$.

Figure 1: China-U.K. and China-U.S. Samples, 1912M04 to 1934M09

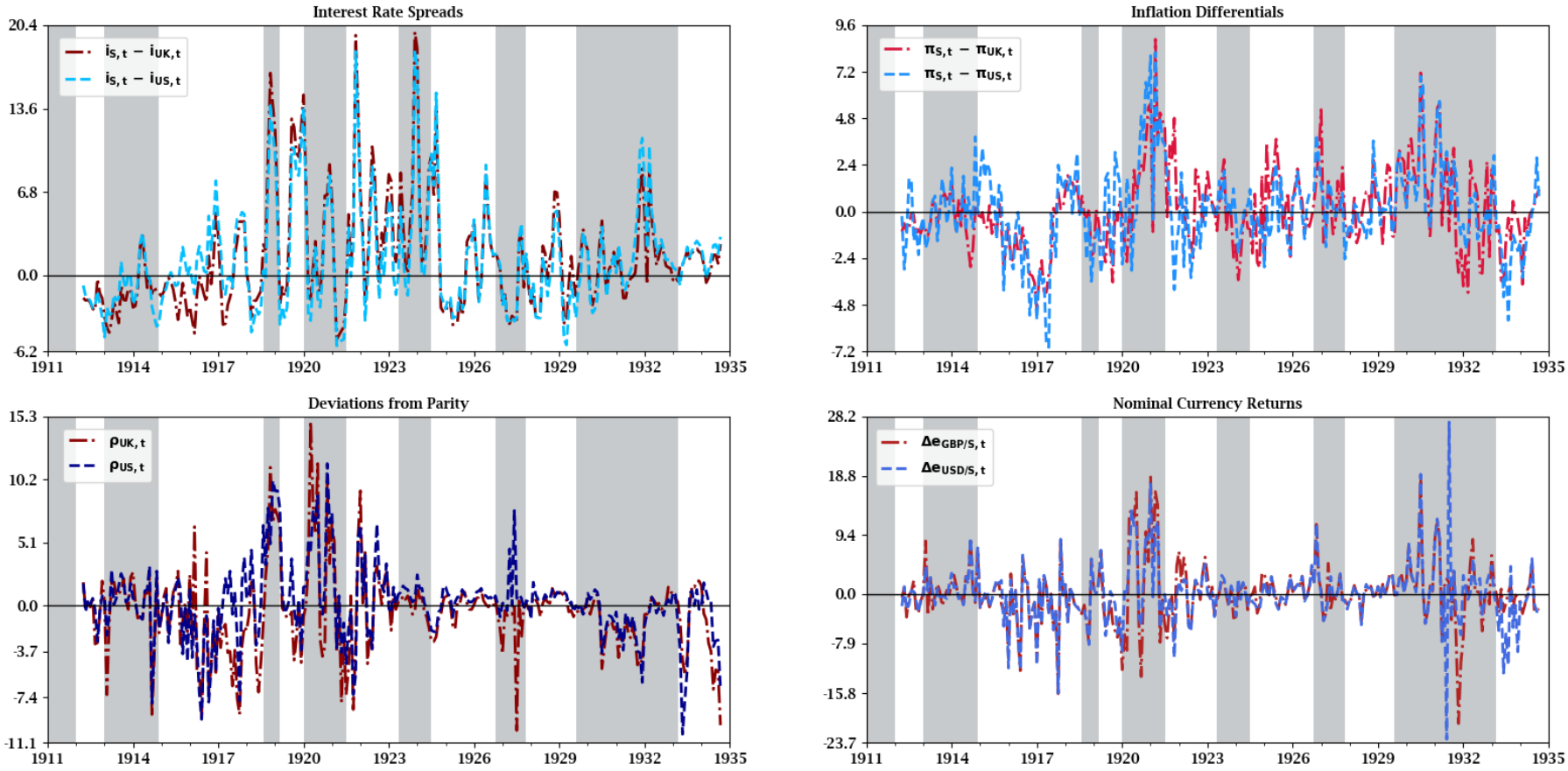

Notes: The top left panel plots the interest spreads, $i_t = i_{S,t} - i_{\ell,t}$, $\ell = UK, US$. Plots of inflation differentials, $\pi_t = \pi_{S,t} - \pi_{\ell,t}$, appear in the top right panel. Risk premiums as deviations from parity, $\rho_{\ell,t}$, are displayed in the bottom left panel. The bottom right panel contains month over month nominal currency returns, $\Delta e_{GBP/S,t}$ and $\Delta e_{USD/S,t}$. The silver shaded vertical bars are NBER dated recessions.

Figure 2: Posterior Moments of the $a_{1:T}$s on the China-U.K. and China-U.S. Samples, 1912M04 to 1934M09

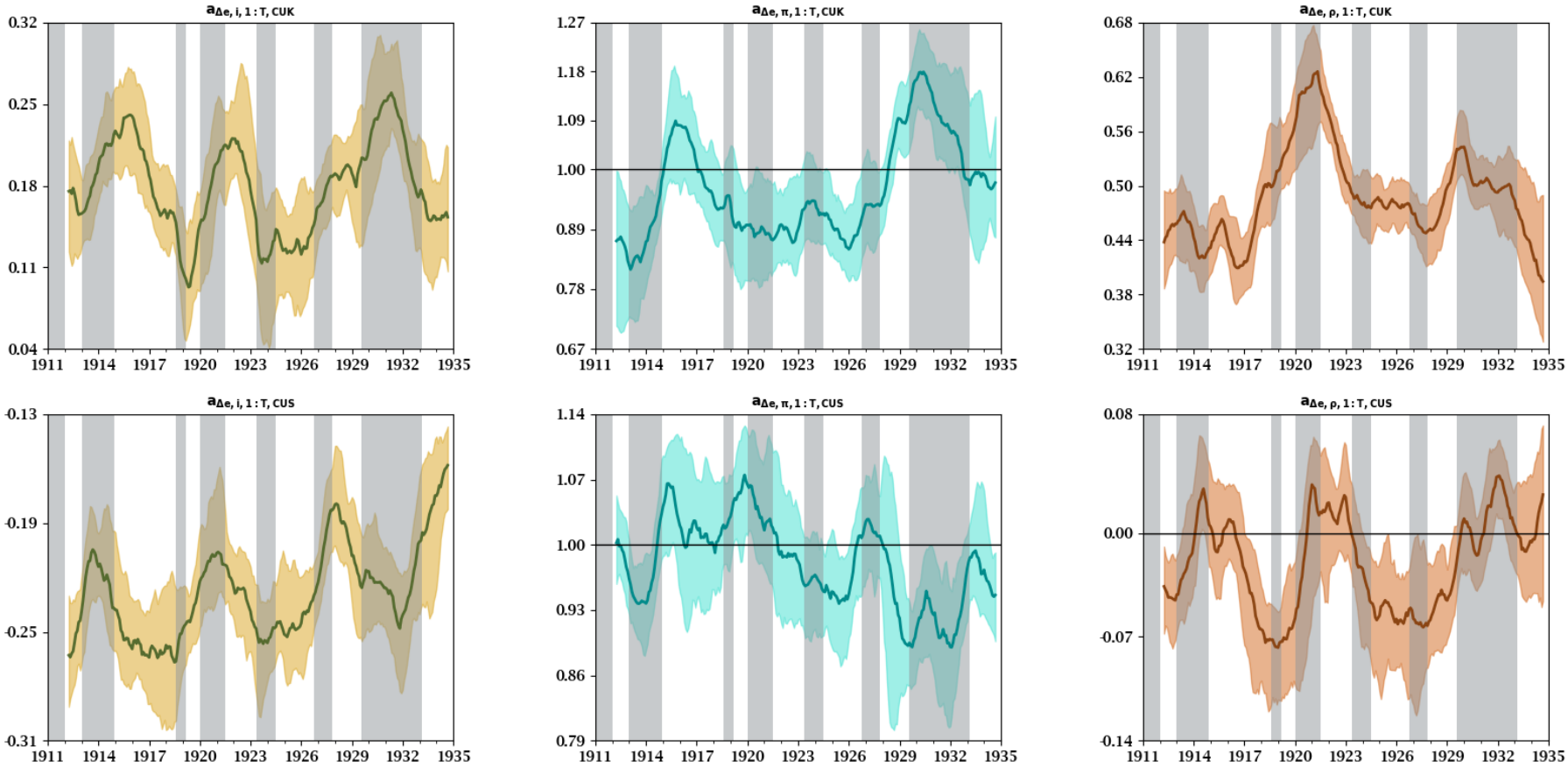

Notes: The panels contain solid lines that are the medians of the posterior distributions of $a_{\Delta e,\, i,1:T,\, j}$, $a_{\Delta e,\, \pi,1:T,\, j}$, and $a_{\Delta e,\, \rho,1:T,\, j}$ conditional on TVP-SV-SVAR-BL and $j = y_{CUK,1:T}$ and $y_{CUS,1:T}$ in the top and bottom rows, respectively. The shadings around the medians of the posterior are 68% Bayesian credible sets (*i.e.*, 16th and 84th quantiles). The silver vertical bars represent NBER recession dates.

Figure 3: Posterior Moments of $y_{1:T}$ on the China-U.K. and China-U.S. Samples, 1912M04 to 1934M09

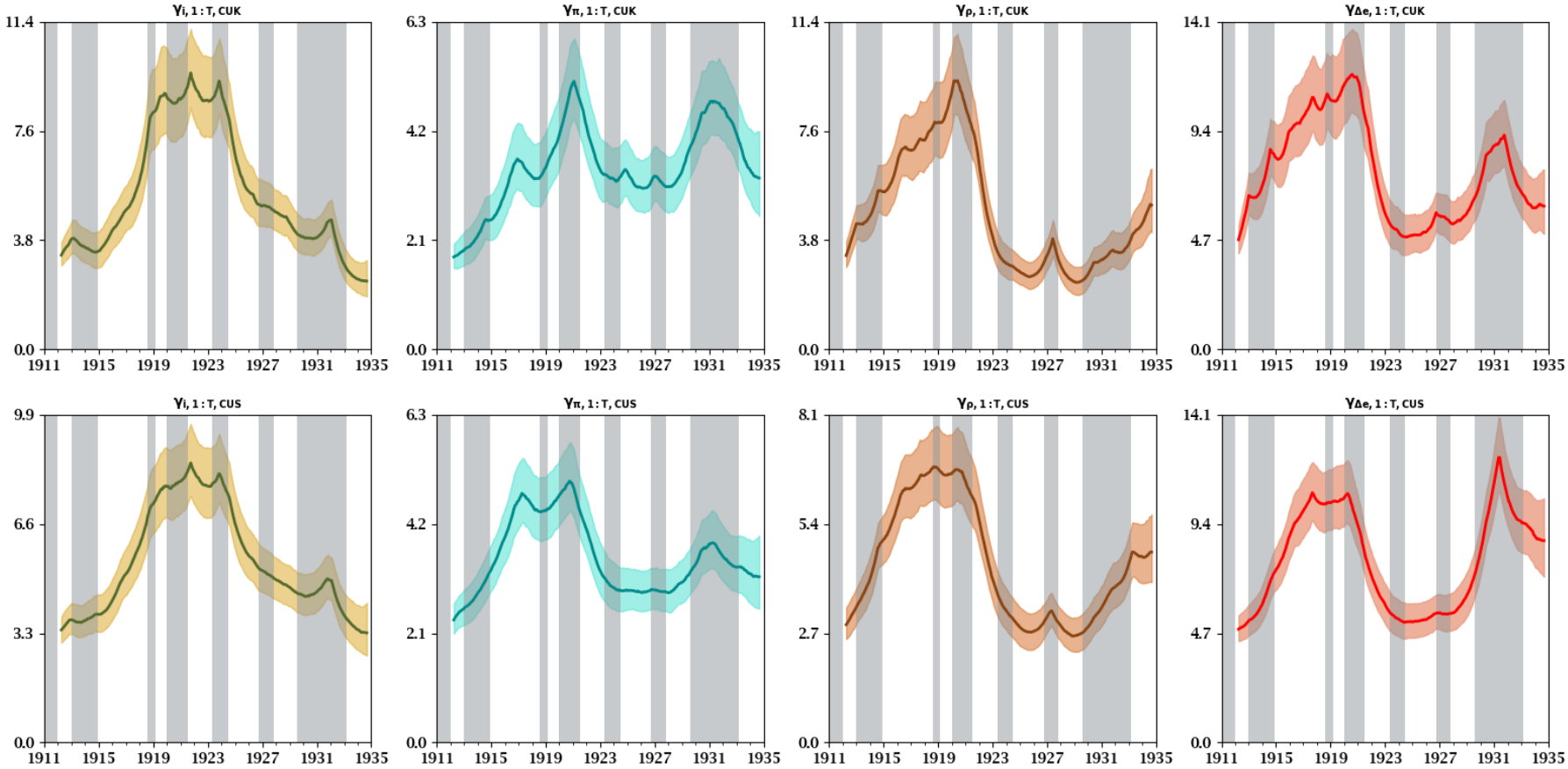

Notes: The top (bottom) row displays panels with solid lines plotting medians of posterior distributions of $y_{j,1:T,CUK}$ $\left(y_{j,1:T,CUS}\right)$ conditional on TVP-SV-SVAR-BL, $y_{CUK,1:T}$ $\left(y_{CUS,1:T}\right)$ and our priors, $j = i, \pi, \rho$, and Δe. The shadings around the posterior medians are 68% Bayesian credible sets. The NBER recession dates are the silver vertical bars.

Figure 4: Slope Coefficients of the Fama and Engel UIP Regressions on the China-U.K. and China-U.S. Samples, 1912M04 to 1934M09

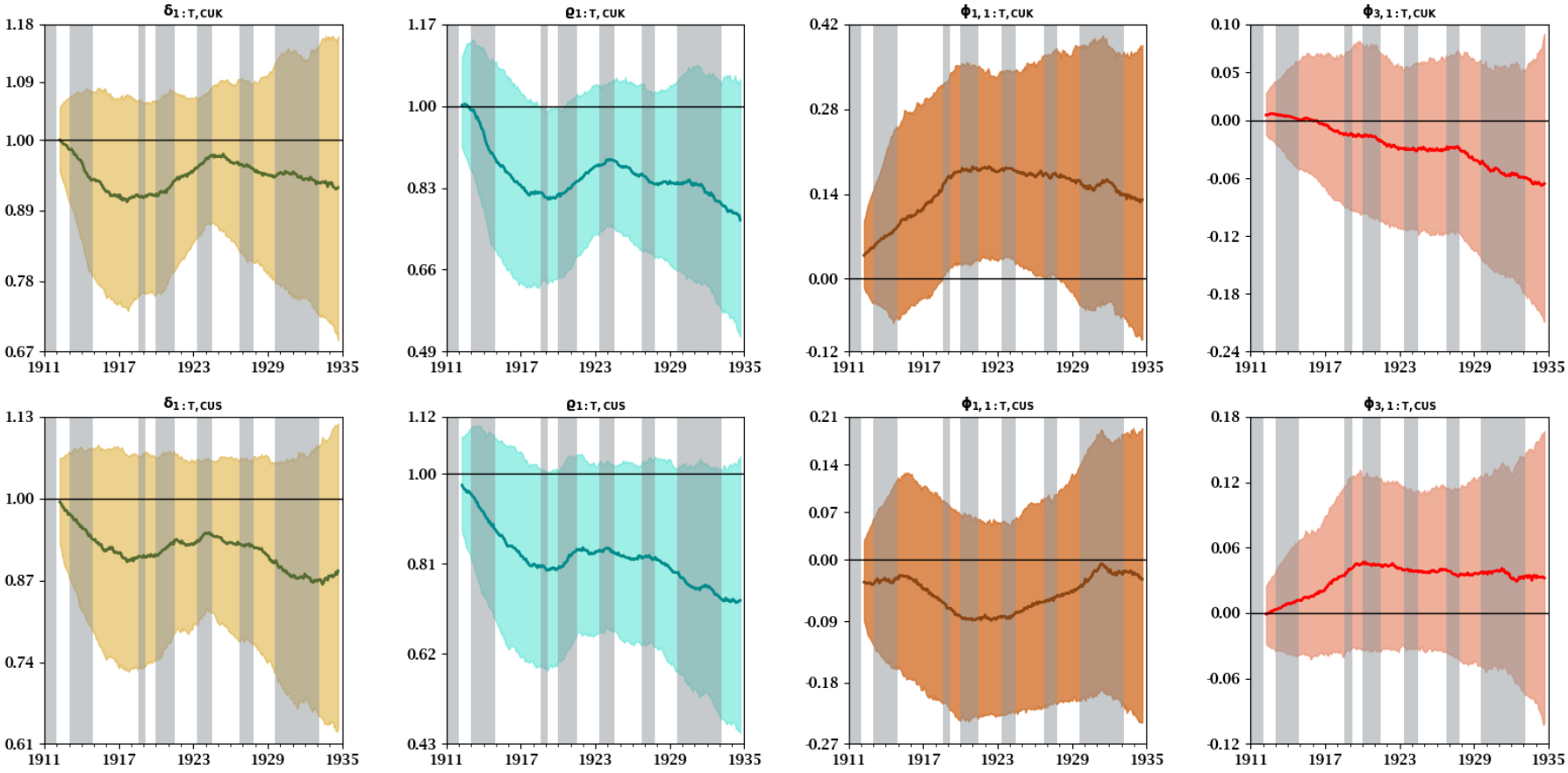

Notes: The figure presents from left to right posterior distributions of the slope coefficients δ_t, ϱ_t, and $\phi_{H,t}$ from regressions of $\Delta e_{t+1} + \left(i_{j,t} - i_{S,t}\right)$ on an intercept and $i_{j,t} - i_{S,t}$, $\Delta q_{t+1} + \left(r_{j,t} - r_{S,t}\right)$ on an intercept and $r_{j,t} - r_{S,t}$, and ρ_{t+1} on an intercept and $\sum_{h=0}^{H-1}\left(r_{j,t-h} - r_{S,t-h}\right)$, where $j = UK, US$ and $H = 1, 3$. The top (bottom) row has slope coefficients computed using the posterior distributions of TVP-SV-SVAR-BL conditional on $y_{CUK,1:T}$ $\left(y_{CUS,1:T}\right)$, and our priors. The solid lines are posterior medians of δ_t, ϱ_t, $\phi_{1,t}$, and $\phi_{3,t}$. The shadings around the posterior medians are 68% Bayesian credible sets. The NBER recession dates are with silver vertical bars.

Figure 5: Posterior Moments of $\mathcal{R}^2_{p,h,1:T}$ and $\mathcal{R}^2_{e,h,1:T}$ on the China-U.K. and China-U.S. Samples, 1912M04 to 1934M09

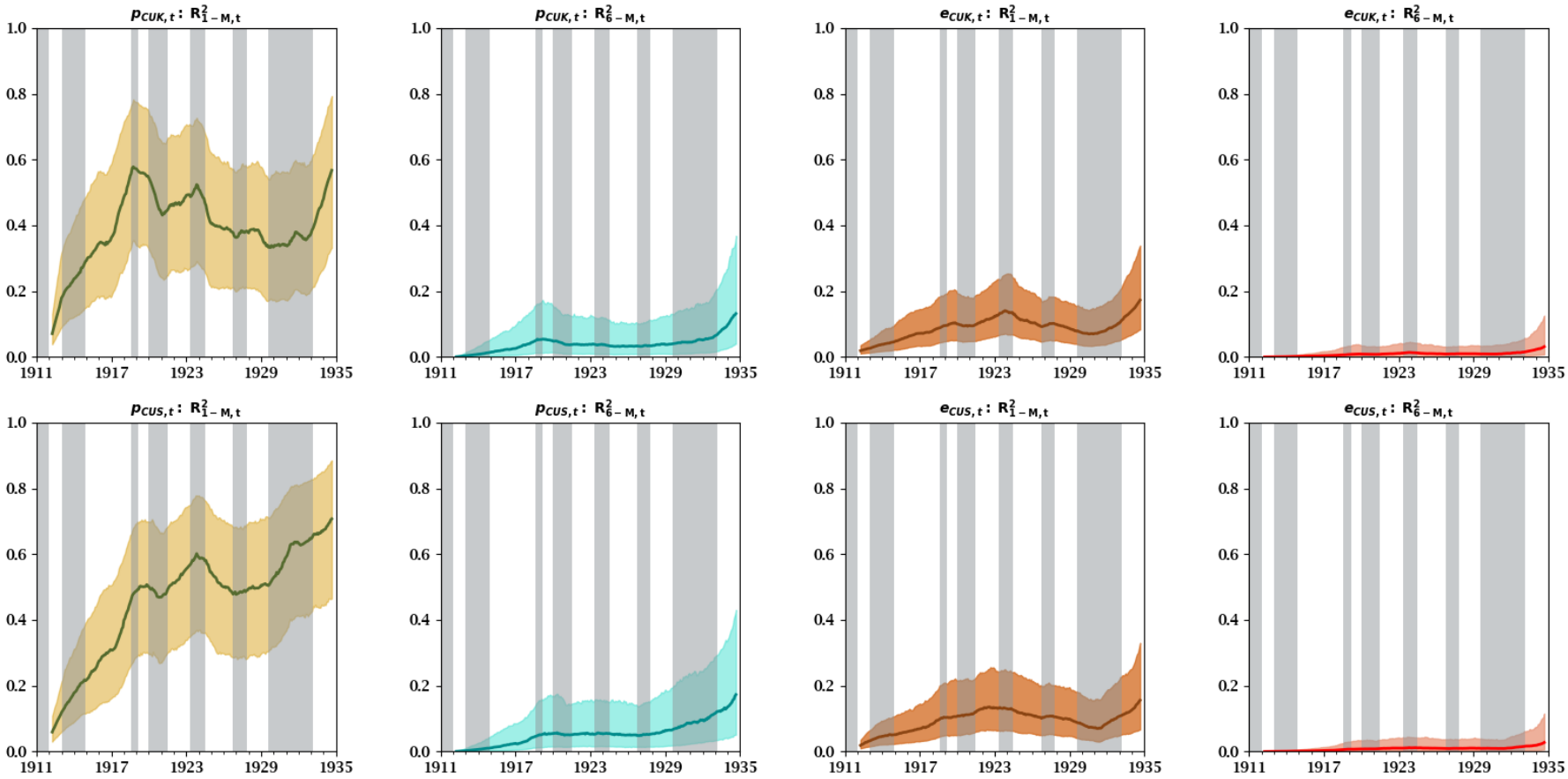

Notes: The top (bottom) row plot the medians of the posterior distributions of $\mathcal{R}^2_{z,1,1:T}$ and the $\mathcal{R}^2_{z,6,1:T}$ produced by TVP-SV-SVAR-BL, $y_{CUK,1:T}$ $\left(y_{CUS,1:T}\right)$, and our priors, where $z = p$ or e. The shadings around the posterior medians are 68% Bayesian credible sets. The NBER recession dates are silver vertical bars.

Figure 6: Posterior Moments of $\sigma_{p,h,1:T}$ and $\sigma_{e,h,1:T}$ on the China-U.K. and China-U.S. Samples, 1912M04 to 1934M09

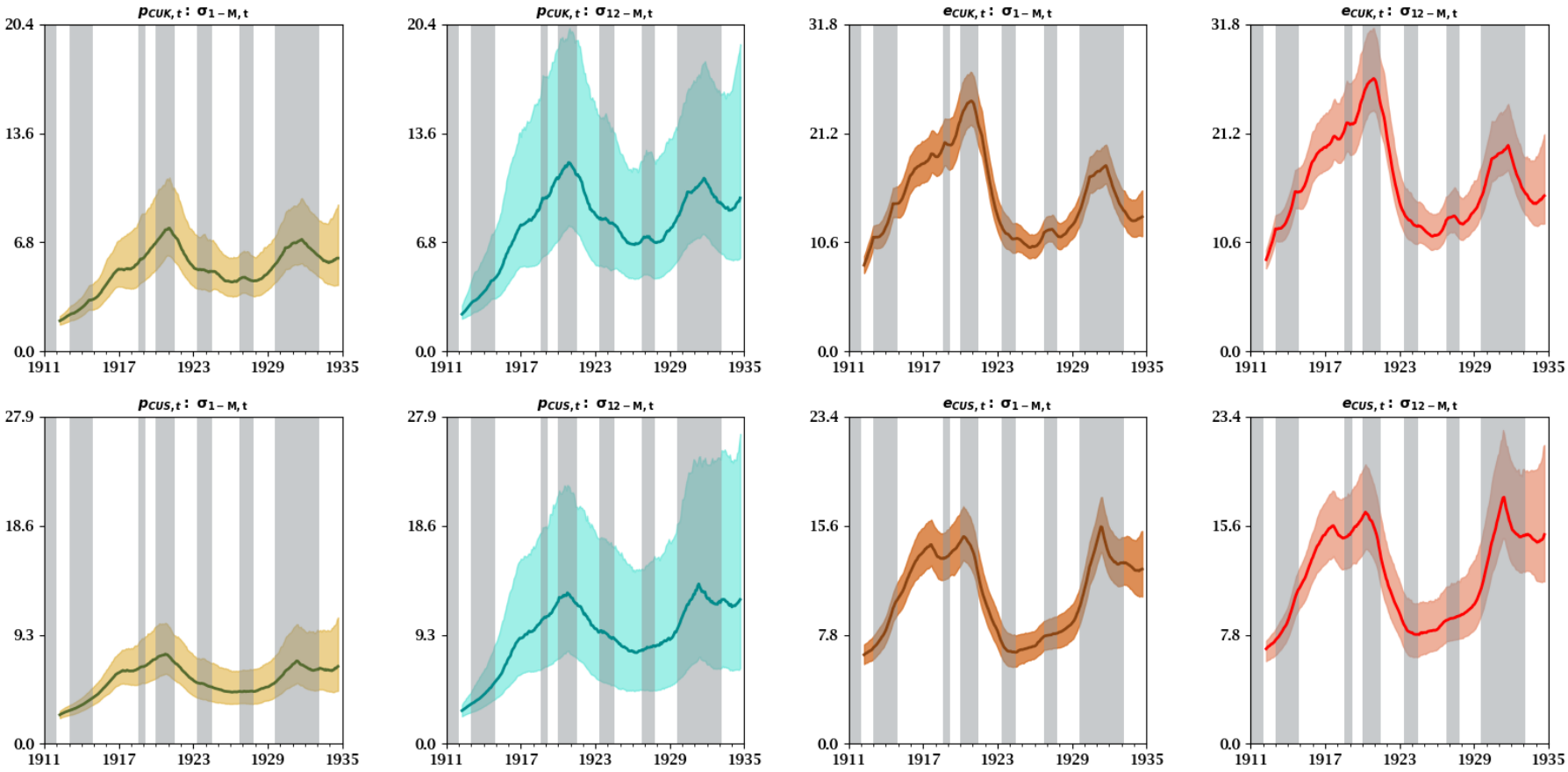

Notes: The top (bottom) row plot the medians of the posterior distributions of $\sigma_{z,h,1:T} = \sqrt{\mathcal{V}_t\left(z_{t+h} - \mathbf{E}_t z_{t+h}\right) + \left(\mathbf{E}_t z_{t+h} - z_t\right)^2}$ produced by TVP-SV-SVAR-BL, $y_{CUK,1:T}$ $\left(y_{CUS,1:T}\right)$, and our priors, where $z = p$ or e, and $h = 1$ and 12. The shadings around the posterior medians are 68% Bayesian credible sets. The NBER recession dates are silver vertical bars.

Figure 7: Impulse Response Functions in 1934 on the China-U.K. Sample

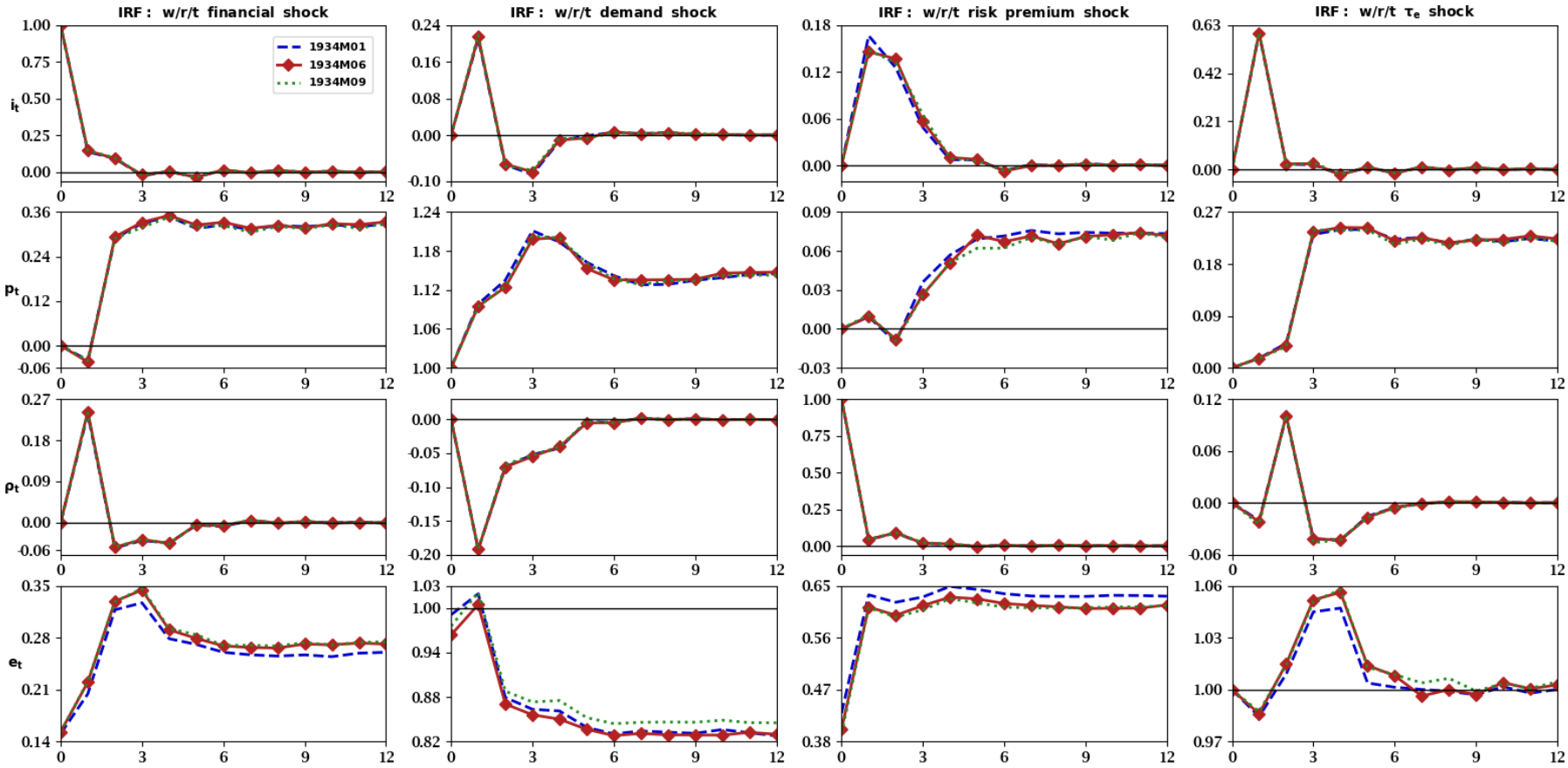

Notes: The top, second, third, and bottom rows display IRFs of i_t, p_t, ρ_t, and e_t at selected dates constructed using the posterior distributions of TVP-SV-SVAR-BL on $y_{CUK,1:T}$ and our priors. From the right to left, the columns show these IRFs with respect to the international financial, cross-country demand, risk premium, and trend exchange rate, $\tau_{e,t}$, shocks. The IRFs run from impact to a 12-month horizon, $h = 0, 1, \ldots, 12$.

Figure 8: Impulse Response Functions in 1934 on the China-U.S. Sample

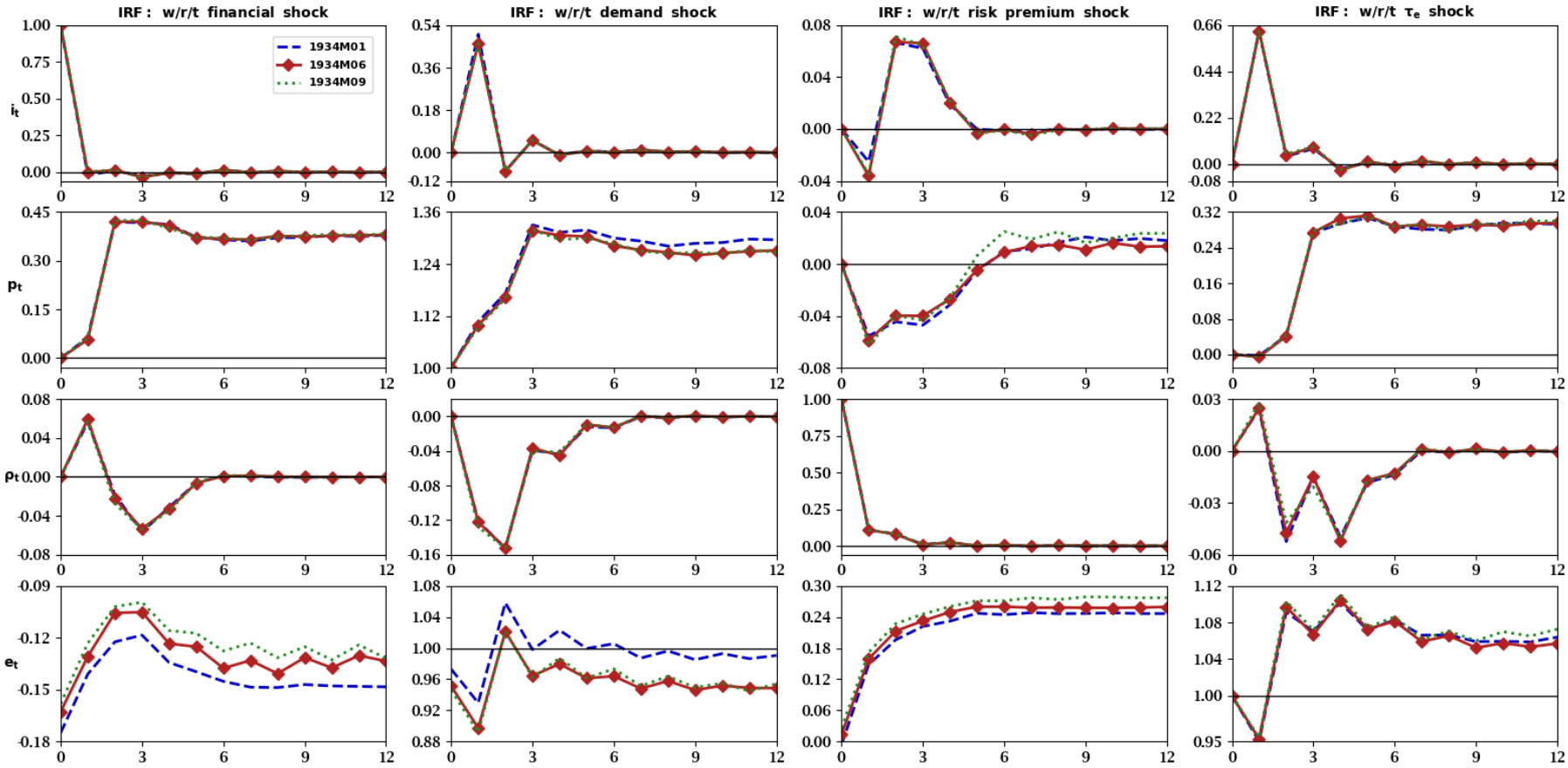

Notes: The top, second, third, and bottom rows display IRFs of i_t, p_t, ρ_t, and e_t at selected dates constructed using the posterior distributions of TVP-SV-SVAR-BL on $\mathcal{Y}_{CUS,1:T}$ and our priors. From the right to left, the columns show these IRFs with respect to the international financial, cross-country demand, risk premium, and trend exchange rate, $\tau_{e,t}$, shocks. The IRFs run from impact to a 12-month horizon, $h = 0, 1, \ldots, 12$.